Retinoblastoma and Hippo pathways cooperate to regulate

cell proliferation and maintain differentiation

BY

BATTUYA BAYARMAGNAI
B.S., University of Wyoming, 2008

DISSERTATION

Submitted as partial fulfillment of the requirements for the degree of
Doctor of Philosophy in Biochemistry and Molecular Genetics
in the Graduate College of the
University of Illinois at Chicago
2015

Dissertation Committee:

Maxim V. Frolov, PhD, chair and advisor

Alisa L. Katzen, PhD

Pradip Raychaudhuri, PhD

Nissim Hay, PhD

Teresa V. Orenic, PhD, Biological Sciences

This dissertation is dedicated to my father J. Bayarmagnai, my mother L. Oyuntsetseg, my aunt J. Alimaa and most of all, to my aunt J. Ariunaa. I thank them for recognizing the importance of education and all their support in my pursuing this degree.

ACKNOWLEDGEMENTS

I thank my advisor, Dr. Maxim V. Frolov, for introducing me to the wonderful world of genetics and for providing me with the encouragement and the means to ask the challenging questions and to go after the challenging experiments. I thank the members of my committee, Dr. Teresa Orenic, Dr. Pradip Raychaudhuri, Dr. Nissim Hay and Dr. Alisa Katzen, for the excellent scientific discussions and challenging me to think deeper. I would like to thank Dr. Alisa Katzen, in particular, for her invaluable advice and input in my scientific and professional development.

I especially would like to thank past and present members of the Frolov lab, Dr. Mary Truscott, Dr. Maria Paula Zappia, Dr. Aaron Ambrus and Dr. Brandon Nicolay, who not only became great colleagues, but also wonderful friends. It's a testament to the friendly environment created in the laboratory where we can also thrive professionally.

I am grateful to our collaborators, Dr. Nuria Lopez-Bigas and Dr. Khademul Islam, for their expertise on bioinformatics. I thank Dr. Brad Merrill for his suggestion to do single cell analysis, and UI-Core for their help in performing the single cell experiments. I thank Dr. Gary Ramsay for his help with confocal microscopy and Dr. Veronique Noguiera for her help with flow cytometry and metabolic assays.

Last, but not least, I would like to thank the *Drosophila* community for their generosity in sharing reagents, fly stocks and protocols. I am grateful to V. Corces, P. Karpowicz, N. Dyson, K. Irvine, J. Lis, K. White, L. Buttitta, I. Salecker, B. Dickson, A. Simcox, T. Orenic, A. Katzen, the Bloomington Stock Center and the Developmental Studies Hybridoma Bank (University of Iowa) for fly stocks and antibodies.

PUBLICATION PERMISSIONS

Chapter 2 was previously published in *Cell Cycle*, a journal of Landes Biosciences. Permission from Landes Biosciences is granted freely, as stated in the License to Publish. Excerpt from the document is below:

> 2. Copyright. Ownership of the copyright remains with the Authors, and provided that, when reproducing all or part of the Contribution, the Authors first acknowledge and reference publication in the Journal, the Authors retain the following non-exclusive rights:
>
> > a. Use of all or part of the Contribution (after publication in the Journal) in any book, article, thesis or dissertation written by the Authors without first requiring permission from Landes.

Part of chapter 3 was previously published in *PLoS Genetics,* a journal of Public Library of Science. Authors retain the copyright of the published material under the Creative Commons Distribution Act.

Author contributions

Chapter	Author	Contribution
Chapter 2	Battuya Bayarmagnai	Figures 3B-N, 4, 5, 6, 7, 8B-D
	Brandon Nicolay	Figure 8A and 8E
	Abul BMMK Islam	Figure 3A

TABLE OF CONTENTS

TABLE OF CONTENTS (Continued)

LIST OF FIGURES

FIGURES PAGE

LIST OF ABBREVIATIONS

APF	After Pupa Formation
Beza	Bezafibrate
ChIP	Chromatin Immunoprecipitation
Co-IP	Co-Immunoprecipitation
DAPI	4,6-Diamidino-2-Phenylindole
dIAP1	Drosophila Inhibitor Of Apoptosis
Doxo	Doxorubicin
dsRNA	Double Stranded RNA
E2f	E2-Promoter Binding Protein
ELAV	Embryonic Lethal Abnormal Vision
Ex	Expanded
Ey	Eyeless
Flp	Flippase
FPLC	Fast Protein Liquid Chromatography
FRT	Flippase Recognition Target
GAF	Gaga Factor
GFP	Green Fluorescent Protein
GMR	Glass Multiple Reporter
HA	Hemagglutinin Tag
Hpo	Hippo
Hth	Homothorax
Mats	Mob As A Tumor Suppressor
MF	Morphogenetic Furrow
mFlp5	Modified Flippase 5
mFRT71	Modified FRT 71
PcG	Ploycomb Group Proteins
PD	Pd0332991
PDAC	Pancreatic Ductal Adenocarcinoma
PI	Propidium Iodide
qRT-PCR	Quantitative Real-Time Polymerase Chain Reaction
Rb	Retinoblastoma
S2	Schneider's Line 2 Cells
Sav	Salvador
Sd	Scalloped
Sens	Senseless
Trl	Trithorax-Like
TrxG	Trithorax Group Proteins
Tsh	Teashirt
UAS	Upstream Activating Sequences
Wts	Warts
Yki	Yorkie

Summary

In efforts to ensure proper development and maintain tissue homeostasis, no signaling pathway functions in isolation. There is a tremendous amount of functional integration. One such example is the cooperation between the Retinoblastoma (Rb) and the Hippo tumor suppressor pathways. We know that the crosstalk occurs on at least two levels: in the regulation of cellular proliferation and in maintenance of terminal differentiation. We uncovered a novel mode of mechanism of the Hippo pathway in cooperation with the Rb pathway to ensure cell cycle exit. The downstream transcription factor complexes, dE2f1/dDP and Yki/Sd, activate the expression of their common target genes. In this work I demonstrate that the chromatin-binding protein GAGA Factor (GAF), is a novel and critical partner in transcriptional regulation by Yki/Sd and dE2f1. I show that functional GAF and its binding to the promoters of target genes common to dE2f1-Yki/Sd is required for both developmental and ectopic cell proliferation.

The differentiation defects following simultaneous inactivation of the Rb and Hippo pathways manifest themselves as the failure to maintain cell-specific markers in the eye imaginal disc. I created a genetic lineage-tracing tool to visualize the cells, which have lost their identity. I optimized the conditions for single cell analysis to determine the mechanism by which Rb and Hippo pathways cooperatively guard the state of terminal differentiation. Initial analysis confirmed the success of our approach and identified mutant cells marked by the expression of the reporter gene *lacZ*. Current experiments of single cell RNA sequencing will give insight into the precise transcriptional signature of the mutant cells.

In light of emerging evidence of the conserved cooperation of the Rb and Hippo pathways, I sought to identify additional points of crosstalk. From studies in both flies and mammals, it is clear that these two pathways control mitochondrial function. Therefore, first I

asked whether therapeutic modulation of the Rb pathway in human breast cancer cells would influence mitochondrial activity. I show that pRb activates mitochondria-associated gene expression in an E2f-independent fashion. This, subsequently, leads to elevated mitochondrial activity and oxidative phosphorylation. Interestingly, enhanced mitochondrial activity sensitizes the normal MCF10A and MCF7 cancer cells to doxorubicin-induced apoptosis, but not the more aggressive MDA-MB-231 cancer cells. This work demonstrates that therapeutic activation of pRb sensitizes cells to apoptosis, but the level of sensitivity varies among cell lines.

1. Introduction

1.1 The Retinoblastoma tumor suppressor pathway

It is widely accepted that a cell needs to undergo multiple lesions in order to become malignant. A cell acquires abilities to evade tumorigenic signals, sustain proliferative capacity, and resist cell death. This is commonly achieved by a deregulation of multiple pathways that govern these processes. Among most frequently found mutations in human cancers are those inactivating the p16/pRB pathway (1). The *Retinoblastoma (Rb)* gene was the first tumor suppressor to be identified (2), and is a key regulator of the cell cycle. Inactivation of the Rb pathway is considered to be an early and obligatory step in cancer progression.

In the absence of mitogenic signals, the hypophosphorylated pRb physically binds to and blocks the activity of the E2f family of transcription factors, targets of which are required for G1 to S phase transition. In response to mitogenic signals, Cyclin Dependent Kinase 4 and 6 (CDK4 and CDK6) phosphorylate pRb, rendering it inactive. Inactivation of pRb permits the progression of the cell cycle. This step is a critical point of regulation, as unchecked E2f activity leads to ectopic proliferation. There is a large amount of experimental evidence underscoring the role of pRb in cell cycle exit (3).

In addition to its key role in guarding the G1 to S phase transition, the Rb pathway has been implicated in many other processes, including DNA damage response, apoptosis, senescence and differentiation (4). Cell cycle exit and differentiation go hand-in-hand as organisms develop. Tumors containing highly proliferative cells, resembling poorly differentiated cells, have been deemed particularly malignant. Mammalian cell culture and mouse tissue-specific Rb knockout studies have revealed an essential role of pRb in differentiation (5,6). In these tissues, the loss of Rb leads to a reduction in the levels of

differentiation markers, apoptosis, and inappropriate proliferation (7). pRb is thought to promote differentiation by cooperating with cell type specific transcription factors. One notable example is where pRb promotes the activity of the CBFA1/Runx2 transcription factor and consequently, osteoblast differentiation (6). This is of particular interest considering the high frequency of pRb inactivation in osteosarcomas (8). However, the precise role of pRb in differentiation remains to be determined.

Studies of the Rb pathway in mammalian systems have proven to be challenging due to the redundant functions of the members of the pRb (pRb, p107, p130) and E2F (E2F1-8) families. In *Drosophila*, there are only two pRb proteins, RBF1 and RBF2, one activator E2F, dE2F1, and a single repressor E2F, dE2F2, yet their functions and roles in the cell cycle are highly conserved (9). Additionally, the diversity of powerful genetic tools available in *Drosophila* makes it an ideal model system for dissecting the function of the Rb pathway.

1.2. The Hippo tumor suppressor pathway

In the last decade or so the Hippo pathway has emerged as one of the major regulators of organ size in *Drosophila* and mammals. The Hippo pathway was first identified and characterized in *Drosophila* (10,11) and subsequently found to be highly conserved in mammalian systems (12-15). A large body of work has shed light onto the inputs and the outputs of the Hippo pathway (Figure 1, adapted from (16)). In response to various signals, the Hippo pathway regulates proliferation, cell survival, metastasis and regeneration (reviewed in (16-19)). The complex upstream regulators include the atypical cadherin Fat, the regulators of the apico-basal polarity, Crumbs, atypical Protein Kinase C and Lethal-giant-larvae, as well as the KEM complex, which comprises Kibra, Expanded and Merlin (reviewed in (20)).

Almost all of these signals converge on the downstream kinase cascade. The core kinase cascade functions analogously in flies and humans (Fig. 1B). In *Drosophila,* Hippo (Hpo) kinase, along with the scaffold protein Salvador (Sav), activates Warts (Wts) kinase, which upon binding to its own partner Mob as a tumor suppressor (Mats) phosphorylates the transcriptional co-activator Yorkie (Yki) (Fig.1B). Yki is phosphorylated on Serines S111, S250 and S168, with S168 being the major sight of negative regulation (21). Phosphorylation on S168 creates a binding site for 14-3-3 protein, which retains Yki in the cytoplasm, rendering it inactive (22). When the Hippo pathway is inactivated, unphosphorylated Yki is free to translocate into the nucleus and upon binding to its DNA-binding partner, Scalloped (Sd) activates its target genes, including *cyclin E*, the miRNA *bantam* and *Drosophila inhibitor of apoptosis (diap1)* (23-25).

A new upstream regulator in the form mechanical tension has been recently identified. This is of significance, because how cells are influenced by the microenvironment is largely not well understood. The response of cells to mechanical cues can dictate cell behavior, and

ultimately determine organ size and shape (26). This is important not only during normal development, but also during cancer formation and metastasis. Two studies in *Drosophila* demonstrated that increased apical F-actin within a cell leads to an increased Yki-driven tissue growth (27,28). Disruption of actin filament assembly by either capping proteins or knockdown of positive regulators of actin polymerization inhibited Yki activity. Similarly, treatment of human HeLa cells with actin de-stabilizing drug Cytochalazin D decreased YAP activity, human ortholog of Yki. They also demonstrated that in addition to responding to actin levels, the Hippo pathway itself may regulate actin levels. This is based on the accumulation of F-actin levels in *ex*, *sav*, *hpo* and *wts* clones. Although these studies described yet another novel aspect of the Hippo pathway, the precise mechanism of this interaction is still not fully understood. However, the Hippo pathway provides the means to connect mechanical tension to tissue growth and organ size. In mammals, the stiffness of the extracellular matrix (ECM) is sensed by the Hippo pathway and results in YAP/Taz transcriptional output (29). Cells grown on hard surfaces exhibited nuclear localization of YAP/Taz. Consistent with their localization, they efficiently activated the expression of their transcriptional reporters. Intriguingly, this regulation of YAP/Taz activity by ECM stiffness is independent of the tumor suppressor kinases, Mst1/2 (Hpo ortholog) and Lats1/2 (Wts ortholog), but requires Rho activity. Collectively, this data from both flies and human cell culture models draw an important connection between extracellular and intracellular mechanical cues and the Hippo pathway transcriptional response.

Consistent with its wide-reaching functions, the Hippo pathway has been implicated in many types of human malignancies. Surprisingly, somatic mutations affecting any members of the Hippo pathway are extremely rare. With the exception of its upstream regulator Mer/NF2 gene, mutations of only a handful of other Hippo pathway genes have been reported; for

instance, a deletion in WW45/Sav in two renal cancer cell lines (30). Instead, tumor suppressor genes of this pathway have been shown to be epigenetically silenced and more generally, the protein levels are observed to be decreased (31). Additionally, increased level of YAP is often correlated with tumorigenesis. Amplification of the *YAP* gene has been reported in a wide variety of cancers, both in human samples as well as in mouse models of cancer. For instance, YAP is overexpressed in ovarian, lung, colorectal, pancreatic and liver cancers (32). Importantly, in a comprehensive study of hepatocellular carcinoma (HCC) patients, 62% (out of 177 tumor samples) displayed high levels of YAP and localized to the nucleus. This overexpression significantly correlated with poor tumor differentiation and poor prognosis for patient survival (33). Collectively, these data highlight the significance of the Hippo pathway in normal development and its implications in pathological conditions.

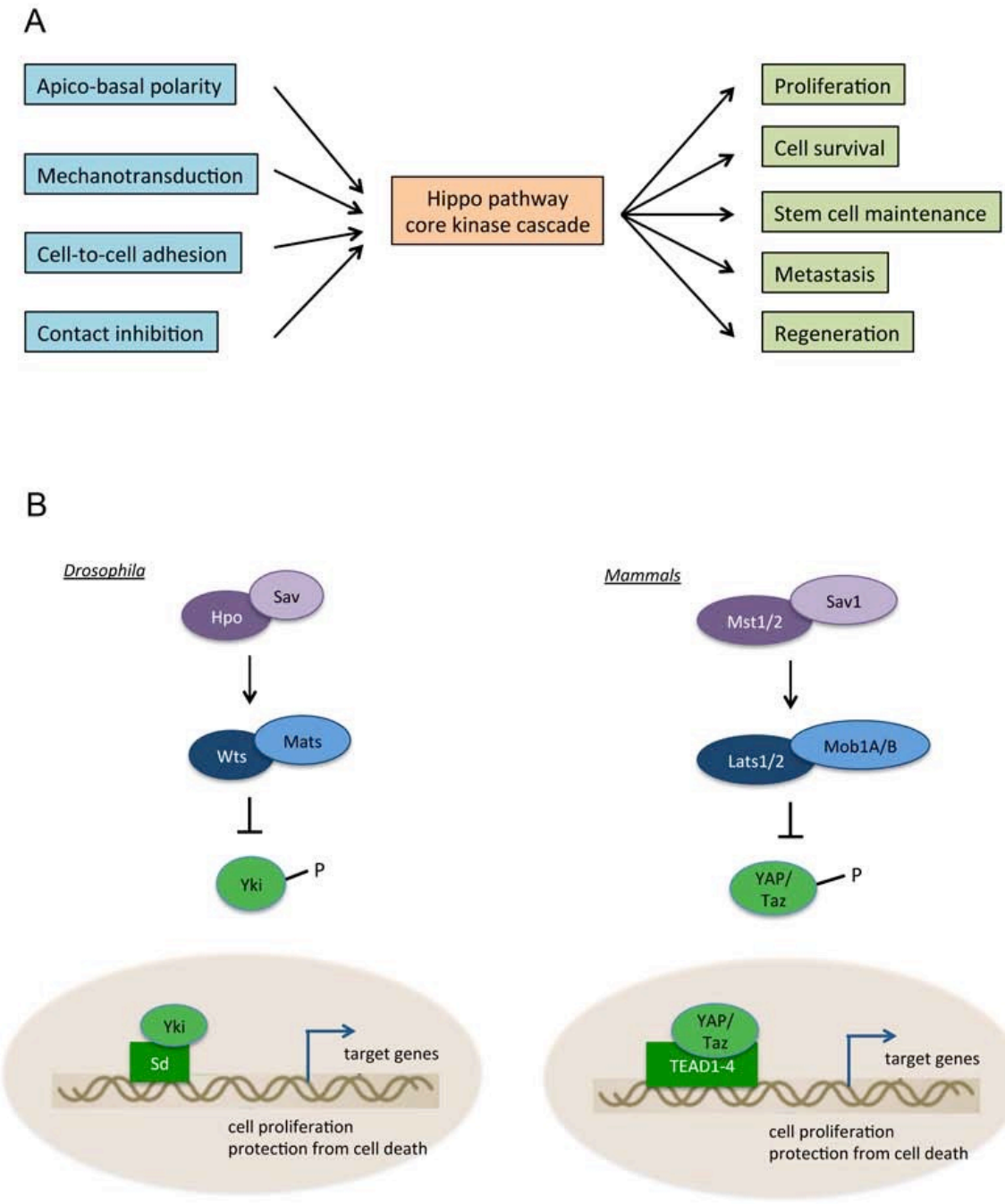

Figure 1. The Hippo tumor suppressor pathway.

(A) Upstream signals, which converge on the core kinase cascade of the Hippo pathway that mediates a variety of downstream processes. Adapted from Harvey K et al (2013).
(B) The core kinase cascade of the Hippo pathway in flies and mammals.

1.3. Cooperation between Rb and Hippo pathways

We previously found that the RBF pathway and the Hippo pathway show a strong genetic interaction. In *Drosophila* retina, where defects in proliferation and differentiation can be easily visualized, we observed that the cells failed to exit cell cycle and have proliferated ectopically. Additionally, the ommatidial clusters containing the photoreceptor R cells failed to maintain their composition and have lost the expression of their photoreceptor markers. The crosstalk occurs on two levels: in regulating cell cycle exit (34) and in regulating differentiation (35). Importantly, the differentiation defects persist in the absence of ectopic proliferation, demonstrating that their roles in proliferation and differentiation are uncoupled and independent of each other (model represented in Fig. 2).

Both Rb and Hippo pathways are critical regulators of cell proliferation. It is intuitive to expect an additive effect on cell proliferation as a result of inactivating two tumor suppressor pathways. However, we observed a synergistic effect and identified a subset of genes, which are direct targets of the downstream effector complexes, dE2f1/dDp and Yki/Sd. The luciferase reporters for these genes were activated only when both complexes were provided, indicative of a synergistic effect of two pathways. This result was further confirmed *in vivo* and with ChIP assays to show that the dE2f1/dDp and Yki/Sd complexes both must be present on the promoters of a subset of common targets to activate the transcription of these genes (34).

Intriguingly, the mammalian field achieved similar conclusions when multiple labs reported the interaction between the Rb and Hippo pathways. In *Kras*-driven pancreatic cancers, tumors often relapse even after *Kras* expression is extinguished. The DePinho lab demonstrated that this relapse relies on YAP1 overexpression, which promotes cell proliferation in cooperation with the E2f transcription factors (36). In another setting, The Sage lab observed that inactivating

all pocket proteins, pRb, p107 and p130 (triple knockout), in hepatocytes triggered a limited proliferative state, which resulted in a stable cell cycle arrest (37). They demonstrated that the sustained proliferative potential is dependent on YAP activity and identified a large number of cell cycle genes to be directly bound by both E2f and YAP. When the hepatocytes were stimulated to proliferate through partial hepatectomy, even in the triple knockout livers, the cells stopped proliferating once the normal size of the liver was reached. Thus, they have identified a mechanism of regulation where organ size sensors override cell cycle regulators. Collectively, these data reveal an important and highly conserved cooperation of the Rb and Hippo pathways in regulating cell proliferation.

As mentioned above, we have uncovered a novel interaction of the Rb and Hippo pathways in differentiation. In a *Drosophila* retina, photoreceptors develop during the third instar larval stage. A snapshot in development reveals a differentiation gradient, which nicely captures asynchronously dividing progenitor cells and differentiating photoreceptor cells as they get specified and mature. We inactivated both pathways by mutations in the tumor suppressor genes *rbf* and *wts.* In both *rbf* single and *wts* single mutants, differentiation is initiated on time and the photoreceptor clusters are morphologically indistinguishable from those in wild type. The cluster composition was visualized by an early marker of differentiation Sens (R8) and the late differentiation marker ELAV (all photoreceptors). The expression of both Sens and Elav is maintained as photoreceptor cells mature. Strikingly, when *rbf* and *wts* were both mutated, the cells failed to maintain the expression of differentiation markers after normal initiation of the differentiation program. This can be concluded from the decrease in the number of Sens and ELAV positive cells while the photoreceptor clusters should be mature. The mechanism of this widespread loss of markers phenotype is not understood.

It is also unclear whether this defect is mediated through the E2f and Yki complexes. Overexpression of the downstream effectors in post-mitotic eye cells does not trigger loss of differentiation markers. However, it is important to note that the E2f and Yki complexes need to be activated earlier in development (i.e. in cycling progenitor cells) in order to conclusively determine their role in maintenance of differentiation markers. Additionally, it must be confirmed whether failure to maintain the expression of differentiation markers is specific to inactivation of the Rb and Hippo pathways.

1.4. Context-dependent binding partners for Yki

The Hippo pathway effector Yki enlists different binding partners to execute its transcriptional output. Commonly, this is achieved by Yki physically associating with various DNA-binding proteins and activating its target genes. The choice of the transcriptional factor depends on the cellular context, such as developmental stage or tissue type. In the wing disc, Yki associates with its main binding partner Scalloped (Sd) (38,39). In the progenitor cells of the eye disc, Yki binds Homothorax (Hth) and Teashirt (Tsh) to promote proliferation and survival, primarily by upregulating miRNA *bantam* (40). With new discoveries, new interacting and DNA-binding partners have emerged. For example, (41) the Irvine lab showed that in order to synergistically promote growth, Dpp and Hippo pathway effectors, Mad and Yki physically bind each other and occupy the enhancer element on the miRNA *bantam* gene.

We and others, revealed a novel mechanism of action where Yki/Sd complex interacts with another effector complex, dE2f/dDP, and bind to the promoters of common target genes. This mechanism we identified in *Drosophila* was later shown to be conserved in mammalian systems, in case of the pancreatic ductal adenocarcinoma and the liver (discussed in detail in 1.3). This is an important mode of action as we try and understand the extent of redundancy and cooperation between signaling pathways.

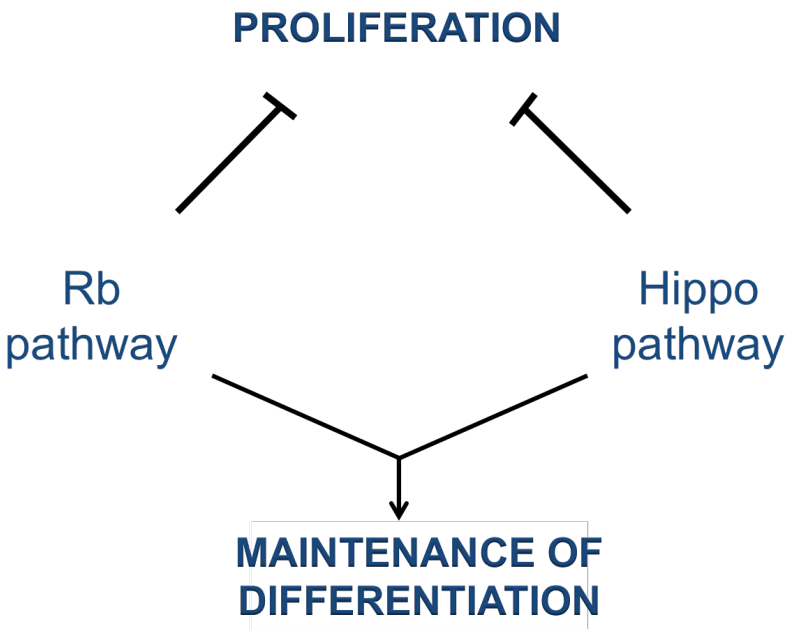

Figure 2. The model for cooperation between Rb and Hippo pathways.

Rb and Hippo pathways cooperate to regulate cell proliferation. Independent of this role, they also cooperate to maintain the identity of terminally differentiated cells.

1.5. Literature cited

1. Hanahan D, Weinberg RA. Hallmarks of cancer: the next generation. Cell. 2011 Mar 4;144(5):646–74.

2. Friend SH, Bernards R, Rogelj S, Weinberg RA, Rapaport JM, Albert DM, et al. A human DNA segment with properties of the gene that predisposes to retinoblastoma and osteosarcoma. Nature. 1986 Oct 16;232:643–6.

3. Chen H-Z, Tsai S-Y, Leone G. RB and E2f: Emerging roles of E2Fs in cancer: an exit from cell cycle control. Nature Publishing Group; 2009 Nov 1;:1–13.

4. Dick FA, Rubin SM. Molecular mechanisms underlying RB protein function. Nature Publishing Group. Nature Publishing Group; 2013 Apr 18;14(5):297–306.

5. Sage C, Huang M, Karimi K, Gutierrez G, Vollrath MA, Zhang D-S, et al. Proliferation of functional hair cells in vivo in the absence of the retinoblastoma protein. Science. American Association for the Advancement of Science; 2005 Feb 18;307(5712):1114–8.

6. Thomas DM. Terminal osteoblast differentiation, mediated by runx2 and p27KIP1, is disrupted in osteosarcoma. The Journal of Cell Biology. 2004 Dec 6;167(5):925–34.

7. Goodrich DW. The retinoblastoma tumor-suppressor gene, the exception that proves the rule. Oncogene. 2006 Aug 28;25(38):5233–43.

8. Feugeas O, Guriec N, Babin-Boilletot A, Marcellin L, Simon P, Babin S, et al. Loss of Heterozygosity of the RB Gene Is a Poor Prognostic Factor in Patients With Osteosarcoma. JCO. American Society of Clinical Oncology; 1996 Aug 1;14(8):2411–1.

9. van den Heuvel S, Dyson NJ. Conserved functions of the pRB and E2F families. Nat Rev Mol Cell Biol. 2008 Sep;9(9):713–24.

10. Udan RS, Kango-Singh M, Nolo R, Tao C, Halder G. Hippo promotes proliferation arrest and apoptosis in the Salvador/Warts pathway. Nature Cell Biology. 2003 Oct;5(10):914–20.

11. Harvey KF, Pfleger CM, Hariharan IK. The Drosophila Mst ortholog, hippo, restricts growth and cell proliferation and promotes apoptosis. Cell. 2003 Aug 22;114(4):457–67.

12. Lu L, Li Y, Kim SM, Bossuyt W, Liu P, Qiu Q, et al. Hippo signaling is a potent in vivo growth and tumor suppressor pathway in the mammalian liver. Proc Natl Acad Sci USA. 2010 Jan 26;107(4):1437–42.

13. Li Z, Zhao B, Wang P, Chen F, Dong Z, Yang H, et al. Structural insights into the YAP and TEAD complex. Genes Dev. 2010 Feb 1;24(3):235–40.

14. Song H, Mak KK, Topol L, Yun K, Hu J, Garrett L, et al. Mammalian Mst1 and Mst2 kinases play essential roles in organ size control and tumor suppression. Proceedings of

the National Academy of Sciences. 2010 Jan 26;107(4):1431–6.

15. Zhou D, Conrad C, Xia F, Park J-S, Payer B, Yin Y, et al. Mst1 and Mst2 Maintain Hepatocyte Quiescence and Suppress Hepatocellular Carcinoma Development through Inactivation of the Yap1 Oncogene. Cancer Cell. Elsevier Ltd; 2009 Nov 3;16(5):425–38.

16. Harvey KF, Zhang X, Thomas DM. The Hippo pathway and human cancer. Nature Publishing Group; 2013 Mar 7;:1–12.

17. Yu FX, Guan KL. The Hippo pathway: regulators and regulations. Genes Dev. 2013 Feb 21;27(4):355–71.

18. Staley BK, Irvine KD. Hippo signaling in Drosophila: recent advances and insights. Dev Dyn. 2012 Jan;241(1):3–15.

19. Halder G, Johnson RL. Hippo signaling: growth control and beyond. Development. 2011 Jan;138(1):9–22.

20. Grusche FA, Richardson HE, Harvey KF. Upstream Regulation of the Hippo Size Review Control Pathway. Current Biology. Elsevier Ltd; 2010 Jul 13;20(13):R574–82.

21. Oh H, Irvine KD. In vivo analysis of Yorkie phosphorylation sites. Nature Publishing Group; 2009 Mar 30;28(17):1916–27.

22. Ren F, Zhang L, Jiang J. Hippo signaling regulates Yorkie nuclear localization and activity through 14-3-3 dependent and independent mechanisms. Developmental Biology. Elsevier Inc; 2010 Jan 15;337(2):303–12.

23. Thompson BJ, Cohen SM. The Hippo Pathway Regulates the bantam microRNA to Control Cell Proliferation and Apoptosis in Drosophila. Cell. 2006 Aug;126(4):767–74.

24. Nolo R, Morrison CM, Tao C, Zhang X, Halder G. The bantam MicroRNA Is a Target of the Hippo Tumor-Suppressor Pathway. Current Biology. 2006 Oct;16(19):1895–904.

25. Huang J, Wu S, Barrera J, Matthews K, Pan D. The Hippo Signaling Pathway Coordinately Regulates Cell Proliferation and Apoptosis by Inactivating Yorkie, the Drosophila Homolog of YAP. Cell. 2005 Aug;122(3):421–34.

26. Low BC, Pan CQ, Shivashankar GV, Bershadsky A, Sudol M, Sheetz M. YAP/TAZ as mechanosensors and mechanotransducers in regulating organ size and tumor growth. FEBS Letters. Federation of European Biochemical Societies; 2014 Aug 19;588(16):2663–70.

27. Sansores-Garcia L, Bossuyt W, Wada K-I, Yonemura S, Tao C, Sasaki H, et al. Modulating F-actin organization induces organ growth by affecting the Hippo pathway. The EMBO Journal. Nature Publishing Group; 2011 May 10;30(12):2325–35.

28. Fernandez BG, Gaspar P, Bras-Pereira C, Jezowska B, Rebelo SR, Janody F. Actin-

Capping Protein and the Hippo pathway regulate F-actin and tissue growth in Drosophila. Development. 2011 May 10;138(11):2337–46.

29. Dupont S, Morsut L, Aragona M, Enzo E, Giulitti S, Cordenonsi M, et al. Role of YAP/TAZ in mechanotransduction. Nature. Nature Publishing Group; 2011 May 30;474(7350):179–83.

30. Tapon N, Harvey KF, Bell DW, Wahrer DCR, Schiripo TA, Haber DA, et al. salvador Promotes both cell cycle exit and apoptosis in Drosophila and is mutated in human cancer cell lines. Cell. 2002 Aug 23;110(4):467–78.

31. Pan D. The Hippo Signaling Pathway in Development and Cancer. Developmental Cell. Elsevier Inc; 2010 Oct 19;19(4):491–505.

32. Dong J, Feldmann G, Huang J, Wu S, Zhang N, Comerford SA, et al. Elucidation of a Universal Size-Control Mechanism in Drosophila and Mammals. Cell. 2007 Sep;130(6):1120–33.

33. Xu MZ, Yao T-J, Lee NPY, Ng IOL, Chan Y-T, Zender L, et al. Yes-associated protein is an independent prognostic marker in hepatocellular carcinoma. Cancer. 2009 Oct 1;115(19):4576–85.

34. Nicolay BN, Bayarmagnai B, Islam ABMMK, Lopez-Bigas N, Frolov MV. Cooperation between dE2F1 and Yki/Sd defines a distinct transcriptional program necessary to bypass cell cycle exit. Genes Dev. 2011 Feb 15;25(4):323–35.

35. Nicolay BN, Bayarmagnai B, Moon NS, Benevolenskaya EV, Frolov MV. Combined inactivation of pRB and hippo pathways induces dedifferentiation in the Drosophila retina. PLoS Genet. 2010 Apr;6(4):e1000918.

36. Kapoor A, Yao W, Ying H, Hua S, Liewen A, Wang Q, et al. Yap1 Activation Enables Bypass of Oncogenic Kras Addiction in Pancreatic Cancer. Cell. Elsevier Inc; 2014 Jul 3;158(1):185–97.

37. Ehmer U, Zmoos A-F, Auerbach RK, Vaka D, Butte AJ, Kay MA, et al. Organ Size Control Is Dominant over Rb Family Inactivation to Restrict Proliferation In Vivo. CellReports. The Authors; 2014 Jul 9;:1–11.

38. Goulev Y, Fauny JD, Gonzalez-Marti B, Flagiello D, Silber J, Zider A. SCALLOPED Interacts with YORKIE, the Nuclear Effector of the Hippo Tumor-Suppressor Pathway in Drosophila. Current Biology. 2008 Mar;18(6):435–41.

39. Zhang T, Zhou Q, Pignoni F. Yki/YAP, Sd/TEAD and Hth/MEIS Control Tissue Specification in the Drosophila Eye Disc Epithelium. Bergmann A, editor. PLoS ONE. 2011 Jul 19;6(7):e22278.

40. Peng HW, Slattery M, Mann RS. Transcription factor choice in the Hippo signaling pathway: homothorax and yorkie regulation of the microRNA bantam in the progenitor

domain of the Drosophila eye imaginal disc. Genes Dev. 2009 Oct 1;23(19):2307–19.

41. Oh H, Irvine KD. Cooperative Regulation of Growth by Yorkie and Mad through bantam. Developmental Cell. Elsevier; 2011 Jan 18;20(1):109–22.

This chapter was previously published

2. GAGA Factor is required for full activation of the E2f1-Yki/Sd transcriptional program

2.1. Summary

The Hippo signaling pathway regulates organ size by controlling the activity of the transcriptional co-activator Yorkie (Yki). Yki is recruited to its target genes by DNA-binding proteins such as Scalloped (Sd). In addition, transcription factor, dE2f1, of the Retinoblastoma (Rb) pathway cooperates with Yki/Sd to synergistically activate a set of common cell cycle target genes. However, little is known about other factors that ensure the proper transcriptional output of Hippo signaling. In this report, we identified the chromatin protein GAGA Factor (GAF), which is encoded by the *Trithorax-like (Trl)* gene, as a novel and critical partner in transcriptional regulation by Yki/Sd and dE2f1. We show that GAF is required for the full activation of target genes by dE2f1 and Yki/Sd; while ablation of GAF compromises both normal and inappropriate cell proliferation driven by Yki and dE2f1 in multiple tissues. The importance of GAF is further supported by strong genetic interactions between GAF and the RB and Hippo pathways. Additionally, we show that GAF directly interacts with RBF, a *Drosophila* Rb homolog, and partially co-localizes with RBF on polytene chromosomes. Collectively, our data provide a novel connection between a chromatin binding protein and a transcriptional program governed by the Hippo and Rb pathways.

2.2. Introduction

How organisms ensure proper organ size and shape is a fundamental biological question. Such mechanisms are important for normal development while their deregulation can lead to malignancy. For example, the Hippo tumor suppressor pathway has been identified as a key regulator of organ size in flies and in mammals. Furthermore, genetic inactivation of the Hippo kinase cascade results in dramatic hyperplasia. In *Drosophila*, a complex network of upstream regulators converges on the core kinase cascade consisting of the Hippo (Hpo) and Warts (Wts) kinases [1,2]. A primary function of this kinase cascade is to regulate the transcriptional co-activator Yorkie (Yki), which mediates the transcriptional output of the Hippo pathway. Following phosphorylation, Yki is retained in the cytoplasm, thus, preventing Yki from executing its transcriptional program. Unphosphorylated Yki translocates into the nucleus and drives the expression of its target genes, many of which are necessary for cell proliferation and protection from apoptosis.

Yki lacks a DNA-binding domain and relies on an array of DNA-binding partners to regulate the expression of distinct target genes. Early studies done in flies identified the TEAD/TEF family protein Scalloped (Sd), the homeodomain protein Homothorax (Hth), and a zinc-finger transcription factor Teashirt (Tsh) [3-5] that recruit Yki to DNA. These proteins were found to help define target gene specificity of Yki in distinct developmental contexts, and, thus, directly influence the output of Hippo signaling. For example, Hth and Tsh promote Yki-dependent cell proliferation and survival in the anterior compartment of the eye imaginal disc by up-regulating the microRNA *bantam* (*ban*) [3]. In contrast, Sd is required for Yki-driven overgrowth in the posterior eye disc and in the wing, although it is not required in the eye during normal development [4,5].

Recent work revealed that two growth control pathways, Decapentaplegic (Dpp) and Retinoblastoma (RB), also directly influence the output of the Hippo pathway [6,7]. In both cases, the output of signaling is dependent on the interaction of Yki with the downstream effectors of the two pathways, Mad and dE2f1 respectively. However, the underlying mechanisms are different. In the case of Dpp signaling, Mad and Yki physically interact to form a transcription factor complex to activate their common targets including the microRNA *bantam* [7]. In contrast, interaction between the RB and Hippo pathways occurs at the level of regulation of a panel of common cell cycle genes such as *DNA polymerase ε*, *Mcm3*, *Mcm10*, and *expanded.* dE2f1 and Yki/Sd bind to distinct DNA elements in the promoters of these genes and synergize in the activation of their expression [6]. The suggested cooperation between dE2f1 and Yki/Sd is supported by genetic interaction tests that showed the *wts* mutant phenotype is strongly enhanced by inactivation of *rbf,* which encodes a negative regulator of dE2f1.

These results illustrate the existence of multiple tiers of regulation that determine the transcriptional output of Hippo pathway signaling. Adding to this complexity, a recent study found that the histone binding protein L(3)MBT co-localizes with three insulator proteins, CP190, CTCF and BEAF-32, to limit the expression of Hippo pathway targets [8]. Insulator proteins affect gene transcription *via* mediating enhancer-promoter interaction and blocking the spreading of heterochromatin [9]. This implies that a dynamic coordination between chromatin factors may exist during Yki-dependent gene activation. Importantly, L(3)MBT has been previously shown to repress E2F-dependent gene expression [10,11]. This prompted us to investigate what influence chromatin proteins have on the regulation of the dE2f1-Yki/Sd transcriptional output.

In this report, we describe GAGA Factor (GAF) as a novel and relevant partner in the transcriptional activation of dE2f1 and Yki/Sd target genes. GAF is encoded by the *Trithorax-like (Trl)* gene [12]. GAF is a multi-functional protein that has been implicated in a variety of biological processes including insulator functions [13,14]. We show that GAF is required for full activation of common targets by dE2f1 and Yki/Sd, while ablation of GAF compromises the ability of Yki and dE2f1 to drive normal and inappropriate cell proliferation. Importantly, GAF is present on dE2f1-Yki/Sd common target promoters and physically interacts with RBF, a negative regulator of dE2f1. Consistently, we observed strong genetic interactions between GAF and the RB and Hippo pathways. Thus, our results provide evidence that GAF is important in ensuring the proper transcriptional output of Hippo signaling.

2.3. RESULTS

A. GAF is required for cell proliferation in the wing

Previous studies have shown that dE2f1 and Yki/Sd synergistically induce the transcriptional program necessary to drive cell proliferation. Chromatin binding and insulator protein GAGA Factor (GAF), which is encoded by the *Trithorax-like (Trl)* gene, is a multifunctional protein that has been shown to play a role in transcriptional activation. To begin to address the role of GAF in transcriptional program driven by Yki/Sd and dE2f1, we selected genes that are up-regulated in *rbf wts* double mutants [6] and then used publically available modENCODE genome-wide location data to identify GAF targets among them. Among 279 genes that were up-regulated in *rbf wts* double mutants, GAF was bound to the promoters of 130 genes. Gene ontology of biological processes (GOBP) enrichment analysis of these gene sets revealed that a statistically significant number of targets of GAF are involved in cell cycle and DNA replication processes (Fig. 3A). Notably, this enrichment profile essentially mimicked the enrichment signature of all dE2f1-Yki/Sd common target genes that we defined previously [6]. Binding of GAF to dE2f1-Yki/Sd targets raises the possibility that GAF may have a role in their regulation. From here on, all the nomenclature in the manuscript, as well as the figures, referring to the gene will be indicated as "*Trl"* and the protein will be designated as "GAF".

We reasoned that if GAF were important for dE2f1- and Yki/Sd-dependent gene expression, then its inactivation would negatively impact cell proliferation. To test this idea, we employed UAS-dsRNA transgenes to reduce the expression of GAF by RNA interference (RNAi) using a *ptc*-Gal4 driver. Within the developing wing, *ptc*-Gal4 is expressed in the narrow domain alongside the anterior-posterior boundary in cells that form the region between the L3 and L4 veins of the adult wings. Reducing cell proliferation within this region, for example by

driving UAS-dE2f1 dsRNA with *ptc*-Gal4, results in narrowing the distance between L3 and L4 [15] and thus, provides a robust qualitative way to assess cell proliferation.

We started by examining the efficiency of GAF knockdown in larval wing imaginal discs of *ptc*-Gal4 UAS-Trl dsRNA by immunofluorescence. As shown in Figure 3B, GAF protein was depleted within the *ptc*-Gal4 expression domain which was visualized with Ptc antibody. Notably, GAF depletion resulted in a significant reduction of the distance between L3 and L4 veins in adult wings (Fig. 3C-E). The decrease of the L3-L4 intervein region could be due to either fewer cells in that region or smaller cell size. Since each intervein cell is marked with a hair in the adult wing, it is possible to distinguish between the effects on cell number and cell size by counting the number of hairs in adult wings. As shown in Fig. 3F-H, the cell density in the L3-L4 intervein regions was indistinguishable between *ptc*-Gal4; UAS-Trl dsRNA and *ptc*-Gal4 control wings. This suggests that the depletion of GAF causes a reduction in cell number in the L3-L4 intervein region. To confirm that reduced proliferation is not transgene specific, we used a different UAS-Trl dsRNA transgene. Expression of this transgene under *ptc*-Gal4 driver efficiently depleted GAF protein and led to a reduction of the L3-L4 intervein region. Furthermore, knockdown of GAF with either of transgenes in the entire wing pouch using the *sd*-Gal4 driver resulted in a severely small and notched wing (Fig. 3I-J). Thus, the reduced size of GAF deficient tissue was observed with two independent UAS-Trl dsRNA transgenes and with two different Gal4 drivers. This strongly argues that GAF knockdown results in reduced cell proliferation in the wing.

B. GAF is required for expression of dE2f1-Yki/Sd targets

Next, we asked whether GAF depletion affects the expression of dE2f1-Yki/Sd targets. We examined the effect of GAF knockdown on the expression of the *ex-lacZ* reporter in the wing imaginal disc. *ex-lacZ* is commonly used to assess Yki-dependent transcription [16,17]. In a wild type wing disc, the *ex-lacZ* reporter is expressed uniformly throughout the wing disc. In contrast, depletion of GAF by RNAi with the *ptc*-Gal4 driver resulted in a slight but consistent reduction in the level of *ex-lacZ* expression in the corresponding domain alongside the anterior-posterior boundary (Fig. 3K).

In a complementary approach, we employed quantitative real-time PCR (qRT-PCR) to measure the expression of a panel of dE2f1-Yki/Sd targets, including *ex*. Total RNA was isolated from larval wing imaginal discs that express UAS-Trl dsRNA under the control of the *sd*-Gal4 driver. As a control, wing discs expressing *sd*-Gal4 alone were used. Consistent with the lower expression of *ex-lacZ* reporter described above (Fig. 3K), the steady state mRNA level of *ex* was found to be reduced (Fig. 3L). Notably, the expression of several tested dE2f1-Yki/Sd common targets was also significantly reduced following GAF knockdown (Fig. 3L). To determine the effect of GAF depletion on expression of other Yki target genes that are not regulated by dE2f1, we examined expression of *diap1* and a microRNA *bantam*, two canonical targets of the Hippo pathway. As expected, overexpression of Yki under control of *sd*-Gal4 driver potently induced their expression (Fig. 3M, N). Interestingly, depletion of GAF with the same Gal4 driver resulted in a subtle but consistent down regulation in the *diap1* mRNA level, while the effect on *bantam* expression was opposite (Fig. 3M, N). Thus, GAF is not only required for the expression of dE2f1-Yki/Sd common target genes, but it appears to be important for the expression of other Yki target(s).

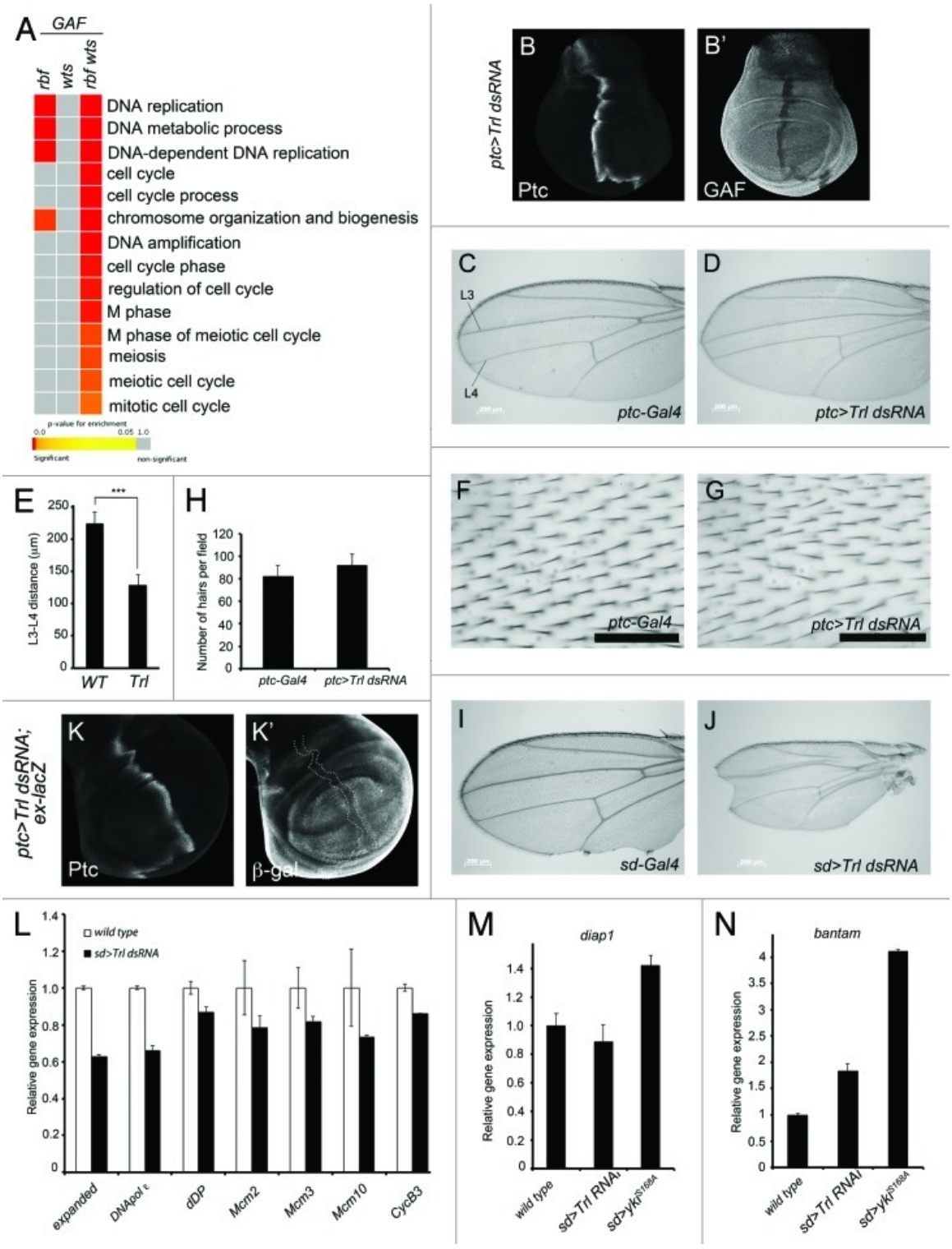

Figure 3. GAF is required for cell proliferation during normal wing development.

(A) Gene ontology biological processes enrichment analysis of GAF targets upregulated in *rbf, wts,* and *rbf wts* double mutant tissue. The red color on the scale indicates statistically significant enrichment, while gray color indicates non-significant categories.
(B) *ptc-Gal4; UAS-Trl dsRNA (ptc>Trl dsRNA)* third instar wing disc stained for Ptc protein (B) and GAF protein (B').
(C) Control *ptc-Gal4* wing with veins L3 and L4 indicated.
(D) *ptc>Trl dsRNA* wing with a reduced distance between veins L3 and L4.
(E) Quantification of the effects of depleting GAF by RNAi on the L3 and L4 distance. Error bars indicate standard deviation from the mean. At least 10 flies were measured per genotype. *** indicates a p-value<0.001.
(F-G) Control *ptc-Gal4* and *ptc>Trl dsRNA* wing regions between veins L3 and L4 to visualize wing hair density. Each hair represents one cell. Size bar corresponds to 50μm.
(H) Quantification of the number of hairs in (F) and (G). Error bars indicate standard deviation from the mean. n=17 (*ptc-Gal4*) and n=9 (*ptc>Trl dsRNA*).
(I) Control *sd-Gal4* and (J) *sd>Trl dsRNA* adult wings.
(K) Expression of *ex-lacZ* in *ptc>Trl dsRNA* background. GAF knockdown is in the Ptc expression pattern, where *ex-lacZ* levels are reduced. The dotted line outlines the area of Ptc expression.
(L) Gene expression levels in *sd>Trl dsRNA* third instar larval wing discs measured by qPCR. The gene levels were normalized to a reference gene, *tubulin*, and shown as fold change relative to *sd-Gal4* control.
(M-N) The levels of *diap1* and microRNA *bantam* expression in wing discs of wild type, overexpressing Yki under the control of *sd-Gal4* driver and *sd>Trl dsRNA*. Error bars represent standard deviation from the mean of technical replicates.

C. *Trl* mutant cells proliferate slowly

To confirm the effects of GAF inactivation by RNAi on cell proliferation, we investigated the phenotype of *Trl* mutant animals. Although *Trl* alleles are embryonic or early larval lethal, some transheterozygous combinations survive until early third instar larvae [16]. We compared wing imaginal discs of Trl^{13C}/Trl^{S2325} transheterozygotes with the wing discs of the heterozygous animals in segregating populations. The Trl^{13C}/ Trl^{S2325} mutant wing discs were markedly smaller than those of the heterozygous counterparts (Fig. 4A' and 3B'). In spite of reduced size, there were no apparent changes in the number of cells in S phases or in mitoses, as revealed by BrdU labeling and staining with antibody against phosphorylated histone H3 (PH3) (Fig. 4A-B). This indicates that *Trl* mutation does not significantly affect different stages of the cell cycle.

To complement these results, the cycling properties of *Trl* mutant cells were quantified in clonal analysis. *hs*-FLP/FRT technique was used to generate mitotic clones of Trl^{13C} mutant cells and their wild type twin spots in the wing disc. Clones were generated at 48 hours after egg deposition (AED) and the wing discs of wandering third instar larvae were dissected 72 hr later. From the individual clone pairs, the areas of Trl^{13C} mutant clone and its wild type sister clone were measured (Fig. 4C). In all of the clone pairs examined, the clone of *Trl* mutant cells was consistently smaller than the wild type sister clone, suggesting that Trl^{13C} mutant cells proliferated slower. Thus, this reduced rate of proliferation is likely to account for the smaller wing disc in the Trl^{13C}/ Trl^{S2325} transheterozygous animals.

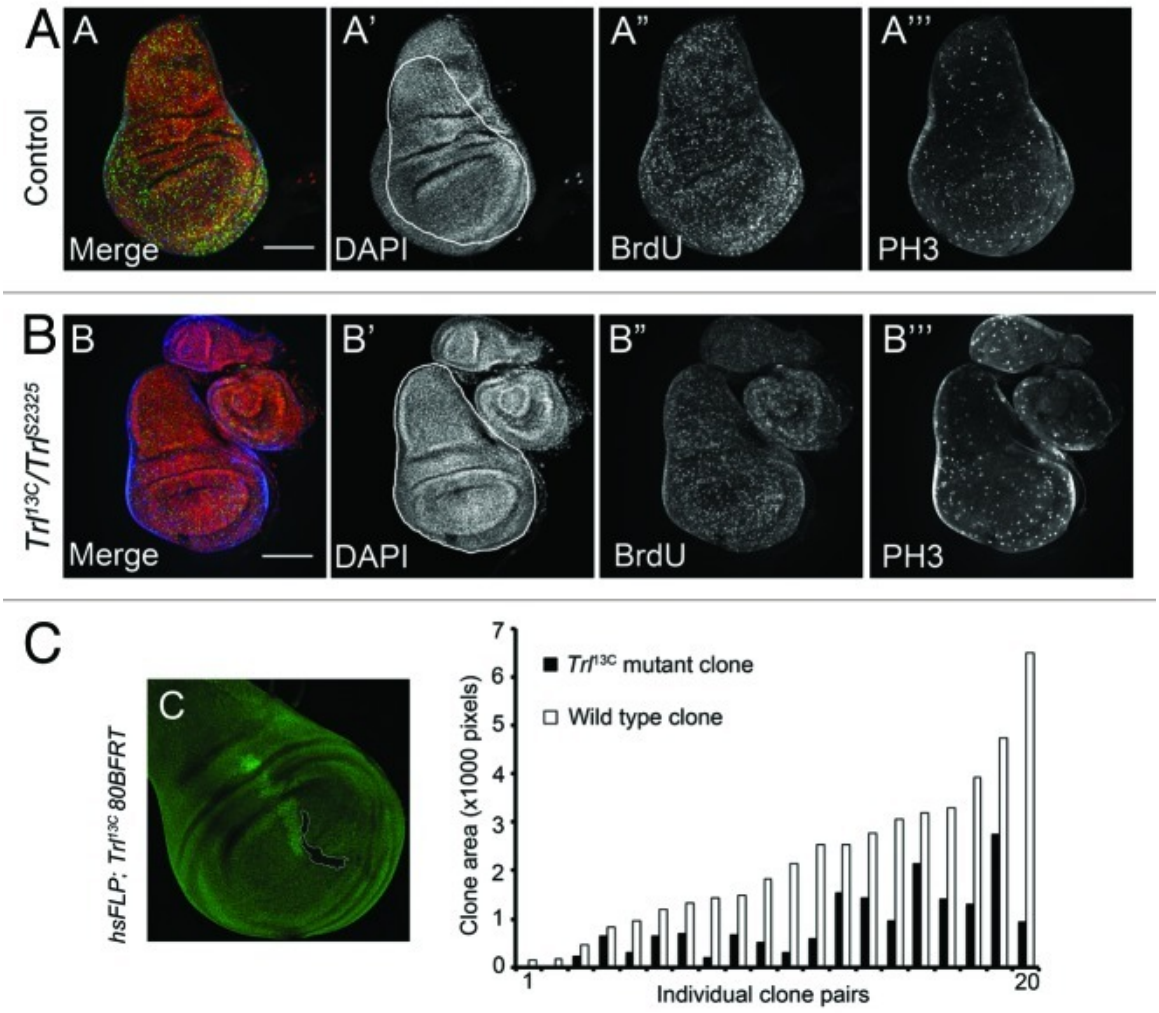

Figure 4.*Trl^{13C}* mutant cells proliferate slowly.

(A) A control third instar wing disc heterozygous for *Trl* stained with DAPI (A'). Cells undergoing S-phase and mitosis are visualized by BrdU and phosphorylated histone H3 (PH3), respectively (A" and A"').
(B) *Trl^{13C}/Trl^{S2325}* transheterozygous wing disc with DAPI, stained for BrdU and PH3. The *Trl^{13C}/Trl^{S2325}* wing disc is outlined with a white line (B') and overlayed onto the control wing disc (A') to demonstrate the difference in the overall size. The size bar is 50μm.
(C) *hs-Flp* induced *Trl^{13C}* mutant clones marked by the absence of GFP expression and outlined. The histogram shows the comparison of 20 pairs of clones with the *Trl^{13C}* mutant clone area indicated with black bars and corresponding wild type sister clones in white bars. The area was measured in pixels using Adobe Photoshop.

D. GAF genetically interacts with the members of the Rb and Hippo pathways

To further understand the functional relationship between GAF and the Hippo and Rb pathways, we performed a series of genetic interaction tests. We first examined the effect of GAF knockdown on Yki-induced growth in the wing. The Wts kinase negatively regulates Yki by phosphorylation on several serine sites. In *Drosophila*, the major regulatory phosphorylation site is Ser168. The mutation of Ser168 to Ala renders Yki constitutively active and hyposensitive to Wts-mediated inhibition [18]. Two additional Wts phosphorylation sites are Ser111 and Ser250. The three Yki phosphorylation mutants: yki^{S111A}, yki^{S250A} and yki^{S168A} have varying levels of hyperactivity, with yki^{S111A} being the mildest and yki^{S168A} being the strongest [19]. Consistently, overexpression of yki^{S111A} and yki^{S250A} using *ptc*-Gal4 led to an expansion of the distance between veins L3 and L4 (Fig. 5A, 5C and 5E, quantification is shown in Fig. 5M), while overexpression of yki^{S168A} resulted in early pupal lethality (Fig. 5G) [19]. In these settings, knockdown of GAF limited the ability of Yki to drive cell proliferation and induce tissue overgrowth. For example, expansion of the region between L3 and L4 induced by yki^{S111A} or yki^{S250A} was suppressed when GAF was depleted in the same domain using UAS-Trl dsRNA (Fig. 5B, 5D and 5F). Furthermore, the depletion of GAF was sufficient to partially rescue the pupal lethality induced by the expression of yki^{S168A} and recover rare escapers (Fig. 5H).

In another assay, we examined the effect of GAF knockdown on Yki-driven proliferation earlier in development in the larval wing imaginal disc. Overexpression of V5 tagged yki^{S250A} under the control of *ptc*-Gal4 driver accelerates cell proliferation as evident by the increased size of the domain of cells expressing Yki when compared to a control (data not shown). However, the depletion of GAF significantly reduced the size of the domain of cells expressing Yki. This reduction was statistically significant and is consistent with the adult wing phenotypes.

Finally, we asked whether GAF genetically interacts with Wts and RBF, the negative regulators of Yki and dE2f1 respectively. As expected, depletion of Wts by RNAi using the *ptc*-Gal4 driver widens the area between veins L3 and L4 (Fig. 5I). The Wts phenotype was potently suppressed by the coexpression of GAF dsRNA (Fig. 5J), in agreement with the requirement of GAF for Yki-induced cell proliferation as described above. GAF also strongly interacted with RBF. RBF restricts cell proliferation by limiting dE2f1 activity. Overexpression of RBF under the control of *ptc*-Gal4 results in a reduced distance between L3 and L4 veins (Fig. 5K and [17]). This phenotype was further enhanced by depletion of GAF (Fig. 5L). Taken together these results suggest that GAF is required for Yki-induced growth and that GAF functionally antagonizes the function of RBF to limit cell proliferation.

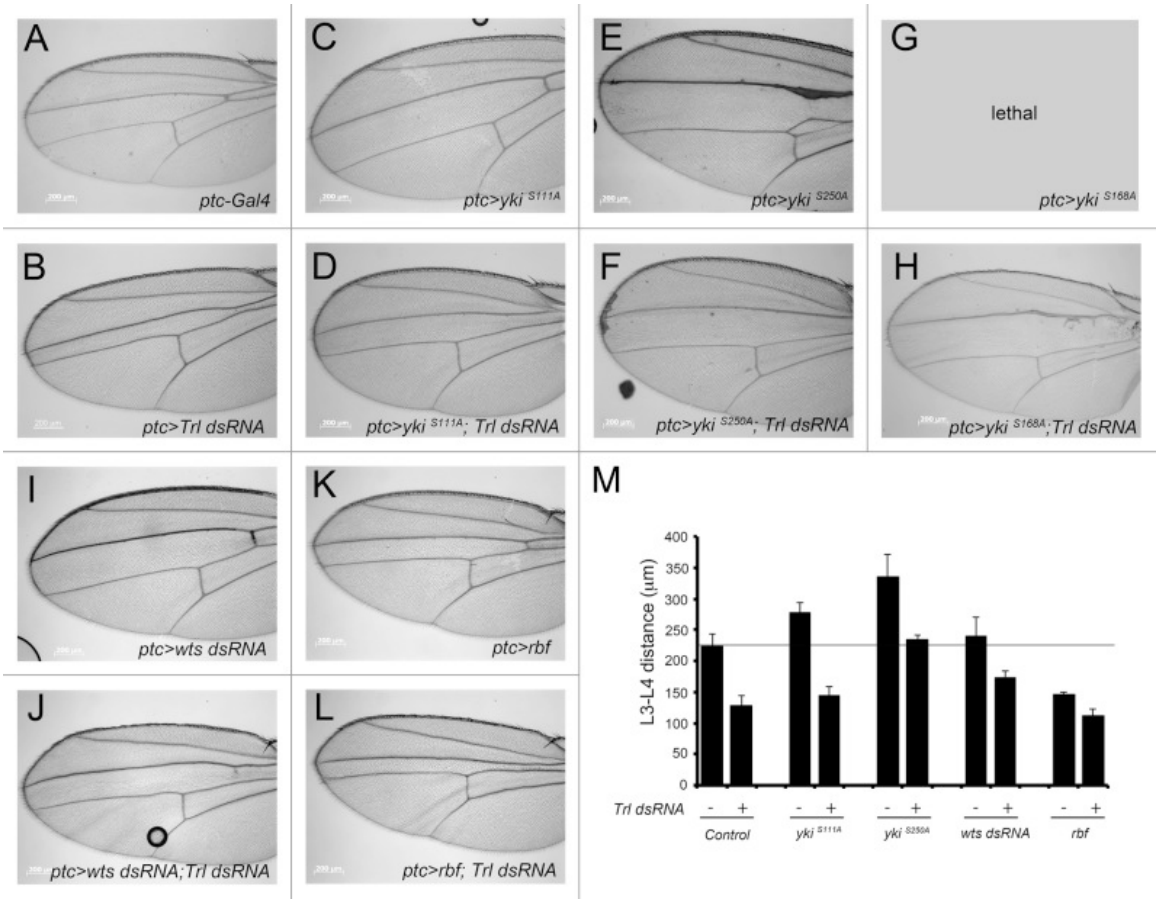

Figure 5. GAF genetically interacts with the members of the RBF and Hippo pathways.

(A) Control *ptc-Gal4* wing.
(B) *ptc>Trl dsRNA* wing with a reduced distance between veins L3 and L4.
(C-J) Depletion of GAF suppresses Yki-induced overproliferation and lethality due to over-expression of *yki* transgenes (C-H) or downregulation of *wts* by RNAi.
(K, L) Depletion of GAF further decreases L3-L4 intervein region that results from over-expressing RBF.
(M) L3-L4 intervein distance measurements for A-L. The horizontal line represents wild type L3-L4 distance. At least 10 adult wings were measured per genotype.

E. The loss of GAF limits inappropriate proliferation driven by Yki

It has been previously shown that the inactivation of the Hippo pathway or overexpression of Yki strongly enhances cell cycle exit defects in *rbf* mutant cells. Such defects are best visualized in the larval eye imaginal disc since cells that have exited the cell cycle are spatially separated from asynchronously proliferating cells. In the wild type eye disc, most cells in the posterior compartment are quiescent and do not incorporate BrdU (Fig. 6A). Overexpression of Yki in the posterior compartment of rbf^{120a} mutant eye discs using a *GMR*-Gal4 driver leads to inappropriate proliferation as evident by the appearance of BrdU positive cells (Fig. 6B). These cells continue to proliferate during the pupal stages leading to ectopic mitoses (marked by PH3) 24 hours after puparium formation (APF) (Fig. 6D-E) and eventually give rise to an excess of interommatidial cells (Fig. 6G-H). Consequently, the distance between ommatidial clusters (marked by Elav) is greatly increased and could be easily visualized in pupal retina 45 hours APF (Fig. 6G-H). Depletion of GAF does not block inappropriate proliferation, as BrdU positive cells are still present in the posterior compartment of rbf^{120a}; $GMR>yki^{S168A}$, Trl dsRNA larval eye discs as well as the PH3-positive cells in the pupal retina 24 hours APF (Fig. 6C and 6F). However, the number of interommatidial cells is partially reduced following GAF knockdown, indicating that the loss of GAF compromises Yki-driven proliferation of rbf^{120a} mutant cells (Fig. 6I and 6J). Interestingly, GAF depletion does not generally compromise cell proliferation in the eye in the context of unperturbed Hippo signaling. For example, RNAi-mediated knockdown of GAF in the eye imaginal disc exerted no effect on the pattern of S phases as detected by BrdU labeling. Consistently, Trl^{13C} homozygous mutant tissue generated by *ey*-FLP was comparable in size with the adjacent wild type tissue and the pattern of mitoses, as revealed by phosphorylated histone H3, remained normal.

To complement this analysis, we determined the effect of GAF knockdown on the expression of a panel of dE2f1/Yki/Sd target genes in rbf^{l20a}; $GMR{>}yki^{S168A}$ mutant eye discs. As expected, overexpression of Yki in the rbf^{l20a} mutant results in up-regulation of dE2f1-Yki/Sd common target genes (Fig. 6K). However, depletion of GAF prevents induction of dE2f1-Yki/Sd targets, suggesting that GAF is required for dE2f1 and Yki/Sd to fully activate their common target genes. These results are consistent with the requirement of GAF for expression of dE2f1-Yki/Sd targets in the wing (Fig. 3).

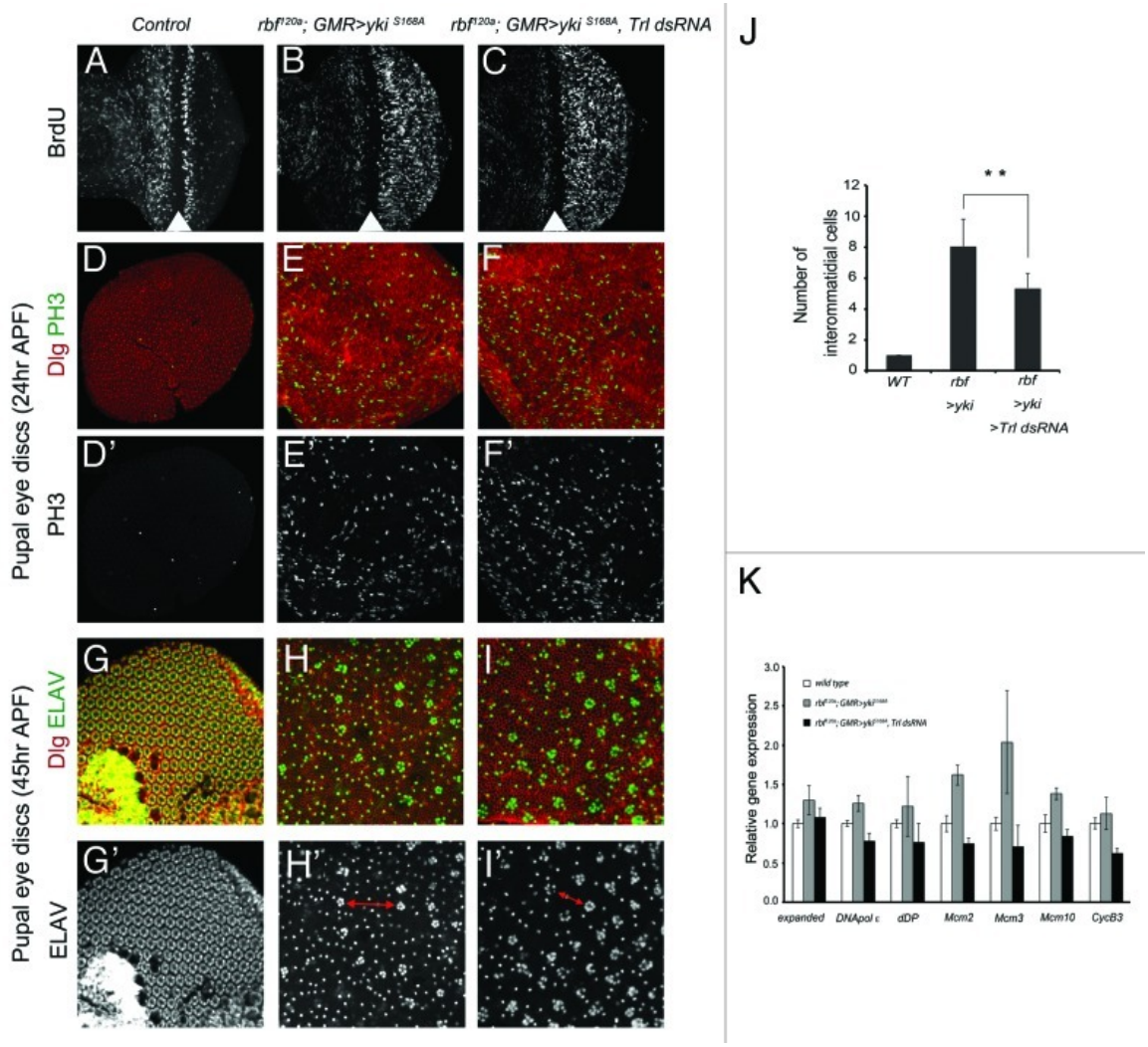

Figure 6. Knockdown of GAF compromises dE2f1- and Yki-driven cell proliferation in the eye.

(A-C) Control *GMR-Gal4, rbf120a; GMR>ykiS168A* and *rbf120a; GMR>ykiS168A, Trl dsRNA* third instar larval eye imaginal discs labeled with BrdU to visualize cycling cells. White arrowhead marks the morphogenetic furrow.
(D-F) Pupal eye discs of the above genotypes were dissected at 24 hr after puparium formation (APF) and stained with Dlg to outline cells and PH3 to mark mitotic cells.
(G-I) Pupal eye discs of the above genotypes were dissected at 45 hr APF and stained with Dlg to outline cells and ELAV to mark photoreceptors.
(J) Quantification of the number of interommatidial cells separating ommatidial clusters in each genotype. The red arrows indicate the distance along which the number of interommatidial cells was quantified. The number of eye discs analyzed are n=5 (wild type), n=5 (*rbf>yki),* n=10 (*rbf>yki, Trl dsRNA).* **indicates a p-value<0.01.
(K) Gene expression levels measured by qPCR in the larval eye imaginal tissues of indicated genotypes.

F. GAF directly binds to common dE2f1-Yki/Sd target genes in vivo

We performed chromatin immunoprecipitation (ChIP) in S2R+ cells to confirm that GAF directly binds to common dE2f1-Yki/Sd target genes. Four representative genes were selected: *DNApol ε*, *dDP*, *Mcm10* and *ex*. As shown in Fig. 7, genomic regions in the proximity of the transcription start site for each gene were strongly amplified in immunoprecipitates with GAF antibody in comparison to a negative control gene *RpP0*. In contrast, no enrichment was found using a non-specific antibody. Consistent with our previous results [6], *DNApol ε*, *dDP* and *Mcm10* genes are also directly bound by RBF, a negative regulator of dE2f1, while the enrichment for *ex* was indistinguishable from the background level.

The results described above raise the question of how many RBF genomic targets are occupied by GAF. Therefore, we examined the *in vivo* genome wide distribution of each of the two proteins by co-staining wild type polytene chromosomes with RBF and GAF antibodies. GAF and RBF each recognize approximately one hundred euchromatic sites on polytene chromosomes [20,21]. As shown in Fig. 8A, GAF and RBF band patterns partially overlap, indicating that the two proteins share a limited number of common sites, although their distributions are distinct.

Since GAF and RBF genetically interact, and appear to participate in the regulation of a shared set of target genes, we tested whether GAF could physically associate with RBF. We started by examining interactions between Flag-GAF and HA-RBF proteins that were transiently expressed in S2 cells. Flag-GAF was significantly enriched in the HA-RBF immunoprecipitates using HA antibody, while only a negligible amount of Flag-GAF was immunoprecipitated in a negative control that lacked HA-RBF (Fig. 8B). Curiously, we observed a modest but consistent

decrease in the levels of HA-RBF upon co-transfection of Flag-GAF (compare input lanes in Fig. 8B).

Next, cells were transfected with a Flag-GAF and the endogenous RBF complexes were immunoprecipitated from the cell lysates. Immunoprecipitates were subjected to Western blotting using Flag antibody. As shown in Fig. 8C, Flag-GAF was detected in the RBF immunoprecipitates, but was absent in a negative control when a non-specific antibody was used for the immunoprecipitation. In a reciprocal experiment, cell lysates were immunoprecipitated with Flag antibody and the presence of endogenous RBF in complex with Flag-GAF was detected by Western blotting with Flag antibody (Fig. 8C).

In cells, RBF can be present either in a free form or in a complex with dE2f. Therefore we asked whether GAF could interact with RBF-dE2f1 complexes. We transiently transfected Flag-GAF and Myc-dE2f1 in S2R+ cells that were treated with a control EGFP dsRNA or with RBF dsRNA to deplete endogenous RBF. As shown in Fig. 8D, Flag-GAF was detected in the Myc-dE2f1 immunoprecipitates from cells treated with a control EGFP dsRNA, but not from RBF depleted cells. This suggests that GAF can interact with RBF that is in a complex with dE2f1.

Finally, to ask whether endogenous RBF and GAF interact, we immunoprecipitated endogenous RBF complexes from S2R+ cells. Immunoprecipitates were separated by SDS-PAGE and Western blot was performed to detect the presence of GAF. Endogenous GAF was specifically detected in the RBF immunoprecipitate, while no signal was observed using a control antibody (Fig. 8E). Importantly, no GAF was found when immunoprecipitation was performed from cells depleted of RBF by RNAi, further confirming the specificity of the interaction. We concluded that GAF associates with RBF under normal physiological conditions.

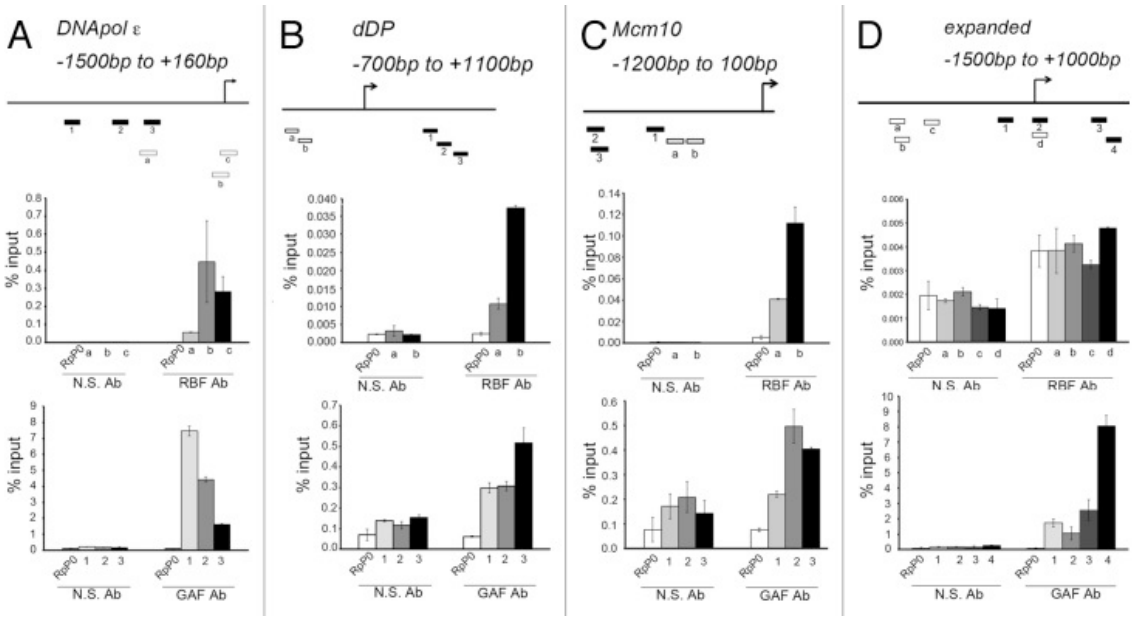

Figure 7. GAF and RBF occupy promoters of target genes common to dE2f1 and Yki/Sd.

Chromatin immunoprecipitation followed by qPCR on *DNApol ε* (A), *dDP* (B), *Mcm10* (C) and *ex* (D). Promoter regions of representative target genes are schematically shown with open bars indicating amplicons for dE2F1-binding sites and closed bars marking amplicons for GAF-binding regions. Antibodies specific to RBF and GAF were used for ChIP. An antibody for MYC epitope was used as a non-specific control. The enrichment was calculated and presented as percent input precipitated with *RpP0* serving as a reference gene.

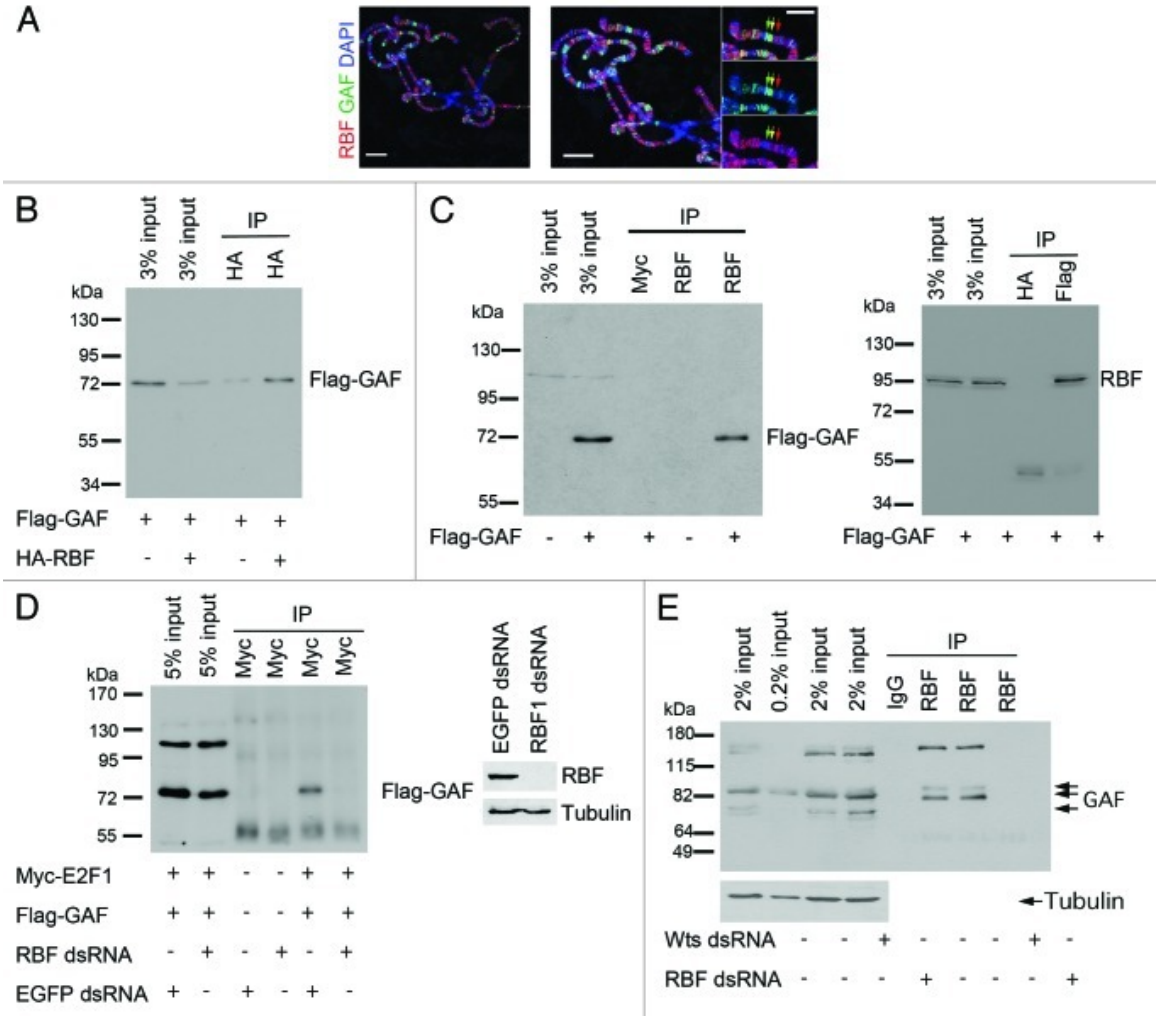

Figure 8. RBF and GAF physically interact.

(A)Distribution of GAF (green) and RBF (red) in *Canton S* wild type polytene chromosomes. DAPI was used to visualize DNA (blue). On the right, red and green arrows point to the bands occupied by RBF only and GAF only, respectively. Yellow arrows point to the bands where RBF and GAF co-localize.
(B) Overexpressed RBF associates with GAF in S2 cells. Cells were transiently co-transfected with plasmids expressing Flag-GAF and HA-RBF. Complexes were immunoprecipitated with anti-HA antibodies. Associated proteins were detected by Western blot analysis with antibodies against Flag. Cells transfected with Flag-GAF only served as a negative control. The molecular mass marker is shown on the left.
(C) Overexpressed GAF and endogenous RBF physically interact. The cells were transfected with Flag-GAF only. Blot on the left shows IP with an antibody specific to endogenous RBF and Western blot for Flag-GAF. An antibody recognizing the MYC epitope was used as a non-

specific control for IP. Blot on the right shows IP with an antibody for Flag tag and Western blot for endogenous RBF. An antibody for HA tag was used as a non-specific control for IP.
(D) Overexpressed GAF associates with E2f1 in S2 cells and this interaction is dependent on RBF. EGFP dsRNA treated control cells or RBF dsRNA treated cells were transiently transfected with plasmids expressing Flag-tag and MYC-E2f1. IP was performed with anti-Myc antibody and the associated protein was detected with anti-Flag antibody. Untransfected cells served as negative control. The molecular mass marker is shown on the left. Western blot for the efficiency of RBF knockdown is shown on the right.
(E) Endogenous RBF and GAF interact in S2 cells. Co-immunoprecipitation followed by western blot demonstrating that endogenous RBF and GAF directly interact. Immunoprecipitation was performed with an antibody specific to RBF followed by Western blot analysis with an antibody specific to GAF. Anti-GAF antibody reveals multiple isoforms associated with RBF. In contrast, no GAF protein is detected when immunoprecipitation was performed from S2 cells that were depleted of RBF by RNAi. Interaction between RBF and GAF is preserved in Wts-depleted cells. Anti-IgG was used as a negative control.

2.4. Discussion

The Hippo pathway is a signal transduction pathway that integrates multiple extracellular cues into a transcriptional output. The focal point of the Hippo pathway is the transcriptional co-activator Yki, which governs the expression of genes needed for cell proliferation and genes that protect from apoptosis. Recent studies have uncovered the existence of multiple tiers of regulation that influence the Yki transcriptional program. One mechanism is defined by the DNA-binding specificity of transcriptional factors such as Sd, Hth, Tsh, and Mad that tether Yki to DNA [3-5,7]. In addition, Yki can cooperate with other transcription factors directly on target promoters. This mode of regulation is exemplified by the synergistic activation of a panel of cell cycle related genes by Yki/Sd and dE2f1 [6]. Here, we report identification of the insulator protein GAGA Factor (GAF) as a novel player in the regulation of dE2f1-Yki/Sd dependent transcription. The failure to fully activate cell cycle target genes in GAF deficient tissues provided a molecular explanation for our findings that dE2f1/Yki/Sd driven cell proliferation is highly sensitive to changes in GAF protein levels.

A requirement for GAF in cell proliferation is particularly evident in the wing pouch where the knockdown of GAF severely compromises growth during normal development. Reduced cell proliferation of GAF deficient cells was observed with two independent UAS-Trl dsRNA transgenes and with two Gal4 drivers. Consistently, *Trl* mutant wing discs were significantly reduced in size, while the clonal analysis revealed that *Trl* mutant cells proliferate much slower than adjacent wild type cells. Taken together, these data strongly argue that the normal function of *Trl* is required for cell proliferation. We note that the results of *Trl* inactivation is reminiscent of the phenotype of *sd* mutants, which similarly exhibit a severe loss of the wing tissue [22]. In contrast, a *sd* mutation does not affect normal proliferation during eye

development, however, it is sufficient to block Yki driven growth in the eye [4,5]. Intriguingly, in a strikingly similar manner, the loss of GAF reduced dE2f1/Yki/Sd driven inappropriate cell proliferation in the eye while exerting no effect during normal eye development. Thus, the genetic interaction between GAF and mutations in the Hippo and RB pathways appears to reflect a specific requirement for GAF for the full activation of the Sd/Yki- and dE2f1-dependent transcriptional program. Given that GAF physically interacts with RBF and partially co-localizes with RBF on polytene chromosomes, we suggest that one of the functions of GAF is to limit or release the inhibitory effect of RBF on dE2f1-Yki/Sd-dependent transcription. In support of this idea, we found that GAF can associate with RBF being in a complex with dE2f1. Although our analysis focused on the role of GAF in expression of dE2f1-Yki/Sd targets, we note that *diap1* and *bantam*, two canonical Yki targets, which are not regulated by dE2f1, were also differentially expressed in GAF deficient cells. Thus, the importance of GAF in Yki dependent transcription could extend beyond genes co-regulated by dE2f1 and Yki/Sd.

GAF belongs to a group of insulator proteins that function by regulating enhancer-promoter interactions and by forming barriers to shield promoters from heterochromatin spreading to regulate gene expression [9]. For example, the only known conserved insulator protein CTCF establishes a chromatin boundary immediately adjacent to the 5' end of the $p16^{INK4a}$ tumor suppressor gene. In the absence of CTCF, repressive chromatin invades the $p16^{INK4a}$ gene and this results in its transcriptional silencing [23]. In *Drosophila*, mutations in the *Trl* gene encoding GAF were initially isolated as enhancers of position effect variegation (PEV) [12]. PEV is the result of a stochastic inactivation of a euchromatic gene when the gene is juxtaposed to centromeric heterochromatin by a chromosomal rearrangement. GAF was shown to counteract the spreading of heterochromatin into the *white* gene in the $In(1)w^{m4}$ inversion by

promoting replacement of heterochromatin associated K9-methylated histones H3 within the *white* gene by histone variants H3.3 [24]. However, it appears unlikely that GAF functions by preventing epigenetic silencing of dE2f1-Yki/Sd common targets, as we did not find an elevated level of me3H3K27, one of the repressive chromatin marks that we tested on these genes upon GAF knockdown (our unpublished observations). Another possibility is that the recruitment of GAF could be affected in the context of Hippo and Rb inactivation, similar to the changes in distribution of insulator proteins following heat shock or ecdysone treatment [25]. However, we did not detect any changes of GAF occupancy on several tested dE2f1-Yki/Sd common targets in RBF depleted cells. Reciprocally, depletion of GAF also did not affect the ability of RBF to occupy the promoters of these genes (our unpublished observations). Thus, although we cannot formally exclude the possibility that GAF relocalizes to different promoters in *rbf wts* double mutant cells, we consider such scenario less likely.

How does GAF contribute to the activation of dE2f1-Yki/Sd target genes? At the *Hsp70* gene locus, one of the best-studied GAF regulated genes, GAF acts by facilitating the formation of a nucleosome free region and helps to maintain the promoter in an open configuration [26]. Loss of GAF significantly compromises the association of the heat-shock factor (HSF) and RNA polymerase with the *Hsp70* promoter [27]. Additionally, GAF was shown to interact with the nucleosome remodeling complexes NURF and FACT to displace nucleosomes and activate gene expression [28,29]. Thus, GAF may stimulate dE2f1 and Yki/Sd-dependent transcription by promoting an open chromatin configuration at their target genes similar to its role at the *Hsp70* promoter.

Interestingly, unlike other transcriptional activators, GAF cannot activate transcription from a naked DNA template. Instead, it can act by counteracting the effects of transcriptional

repressors [30]. In this respect, our findings that GAF physically interacts with RBF, a negative regulator of dE2f1, is particularly intriguing. RBF was shown to block synergistic activation by dE2f1 and Yki/Sd in transcriptional assays [6]. Although the precise details of how RBF limits dE2f1-dependent transcription in *Drosophila* are not known, one of the mechanisms by which the mammalian ortholog pRB blocks E2F activation, is by interfering with early stages of the preinitiation complex formation [31]. The physical interaction between GAF and RBF that we report here raises the possibility that GAF may relieve the inhibitory effect of RBF on dE2f1 activation. Such an idea is consistent with our observed partial colocalization between GAF and RBF on polytene chromosomes. While this study focuses on dE2f1-Yki/Sd target genes repressed by RBF, it is tempting to speculate that GAF may enhance the activation of other RBF-independent Yki transcriptional programs, such as those activated in concert with Hth or Tsh or Dpp signaling. This idea is consistent with our finding that a non-dE2f1 dependent Yki target *diap1* is down-regulated following GAF depletion. Future studies will be necessary to identify the influence of GAF activity on these transcriptional outputs.

2.5. Materials and Methods

A. Fly Stocks

The following transgenic UAS-dsRNA (RNAi) lines were provided by the Vienna Drosophila RNAi Center (VDRC): RBF RNAi (ID 10696), wts RNAi (ID 9928), Trl RNAi (ID 41095, ID 106433). UAS-yki [19] and ex-lacZ [16] lines have been previously published. UAS-RBF is a gift from N. Dyson. The following transgenic recombinants were generated for the final analysis: ptc-Gal4; Trl dsRNA.

B. Chromatin Immunoprecipitation

ChIP was performed as described in [6]. Chromatin was immunoprecipitated with the following antibodies: mouse anti-Myc (9E10, 1:100), mouse anti-RBF (DX3/DX5, 1:10) and rabbit anti-GAF (K.White, 1:1000). The amount of immunoprecipitated DNA was measured by quantitative PCR (Roche LightCycler 480 II) using the standard curve method and presented as percent input.

C. Immunofluoresence

Antibodies used were mouse anti-Ptc (DSHB, 1:50), rat anti-ELAV (DSHB, 1:150), mouse anti-Dlg (DSHB, 1:400), mouse anti-BrdU (Beckton Dickinson, 1:50), rabbit anti-PH3 (Millipore), mouse anti-β-gal (DSHB, 1:200), Cy3- and Cy5-conjugated secondary antibodies (Jackson ImmunoLaboratories, 1:200). The cells were also stained with DAPI (Sigma). Larval and pupal tissues were fixed in 4% formaldehyde for 30 min on ice, washed in phosphate-buffered saline and 0.3% Triton X-100 (PBST) and incubated with the primary antibodies overnight in PBST and 10% normal donkey serum. The samples were incubated with the secondary antibodies for

1hr at RT at the concentration of 1:200. The imaginal discs were then washed in PBST and stored in glycerol with propyl gallate anti-fade reagent. The images were captured using the Zeiss LSM700 confocal microscope.

D. qRT-PCR

Total RNA was extracted from larval imaginal discs (~30 discs per sample) in TRIzol (Invitrogen) and precipitated with isopropanol at -20^{o}C. The RNA was re-suspended in ddH_2O. Reverse transcriptase PCR (RT-PCR) was performed using iScript kit (BioRad) according to the manufacturer's instructions. qPCR was performed using Roche reagents on a Roche LightCycler 480 II machine. The gene levels were calculated using the standard curve method and normalized to the reference gene.

E. Polytene chromosomes

The salivary glands were dissected in phosphate-buffered saline and placed in the fixation solution (4% Formaldehyde, 45% acetic acid) for 1-2 min. The chromosomes were squashed between a microscope slide and a coverslip, and then snap frozen in liquid nitrogen. The coverslip was removed and the sample was washed in PBS+ 1% Triton X-100 for 10 min. Following the wash step, the samples were incubated in the blocking solution (1xPBS, 5% dry milk, 0.2% Tween-20) for at least 1 hr and then rinsed in 1xPBS for 3-5 min. For antibody labeling, the samples were placed in a humidified chamber, covered with 30-40 ml of blocking solution containing the primary antibody. The antibodies used were mouse anti-RBF (DX3, 1:25) and rabbit anti-GAF (a gift from J. Lis, 1:300). The coverslips were placed on glass slides and the humidified chamber was placed at 4^{o}C overnight. The samples were washed twice in 1xPBS

for 5 min each on the rocker and were incubated in the blocking solution containing secondary antibodies in the humidifier chamber for 1 hr at RT and protected from light. Then, DAPI was added to stain DNA and incubated for additional 20 min. After that, the samples were washed in Solution "300" (1xPBS, 0.3M NaCl, 0.2% NP-40, 0.2% Tween-20) for 15 min followed by a wash in Solution "400" (1xPBS, 0.4M NaCl, 0.2% NP-40, 0.2% Tween-20) for 15 min. The samples were covered with the mounting media and a coverslip.

F. Immunoprecipitation-Western

The cDNA for Trl-PC isoform of GAF was cloned with a Flag tag into pIEX-7 Ek/LIC vector (Novagen). For IP-Western with epitope-tagged proteins, the cells were transfected with 3g of plasmids expressing tagged proteins and incubated for 48 hrs at 25^{o}C. Antibodies used are mouse anti-HA (1:10 for IP) and rabbit anti-Flag (Sigma, 1:7000 for WB). The IP was performed overnight at 4^{o}C, after which the lysates were incubated with 20g Protein G:A (1:19) Sepharose beads for mouse antibodies or 20g Protein A Sepharose beads for rabbit antibodies.

In order to perform IP through endogenous RBF and blot for transfected Flag-GAF, we pooled monoclonal antibodies for RBF (DX3 and DX5, 1:10 each for IP) and blotted the membrane with rabbit anti-Flag (Sigma, 1:7000). For IP through Flag-GAF, rabbit anti-Flag Ab (Sigma, 1:300) was used and the immunoprecipitated endogenous RBF was detected with mouse anti-RBF Ab (DX5, 1:250).

For the experiments with RNAi-mediated knockdown of RBF, the cells were incubated with 50g of dsRNA targeting RBF1 in serum-free media for 4 hrs, after which Schneider medium containing 10% FBS was added. The protein depletion lasted 96 hrs and these cells were transfected with indicated plasmids and incubated for additional 48 hrs. co-IP followed by

Western blot was performed as described above with the exception of using Dynabeads (Invitrogen).

Immunoprecipitation followed by Western blot for endogenous proteins was performed using $2x10^8$ *Drosophila* S2R+ cells per IP and as described previously [6]. The lysate was immunoprecipitated with either a mouse RBF monoclonal antibody (DX5, 1:5) or a mouse IgG (1:500) as a nonspecific control. Membranes were probed with rabbit anti-GAF antibody (a gift from J.Lis, 1:2000) and with mouse anti-E7 (β-tubulin, 1:10000) as a loading control for input.

G. Adult wing analysis

Adult flies were dehydrated in 100% ethanol for at least 24 hours. The wings from female flies, unless otherwise indicated, were plucked and mounted on a glass slide and immersed in the mounting medium (Permount, Fisher). L3-L4 vein distance measurements were calculated using Adobe Photoshop tools and normalized to the scale. A one-tailed, paired, Student's *t*-test was performed to draw statistically significant comparisons cited in the figure legends.

H. Clonal analysis in the wing disc

The clones were induced 48 hrs after egg deposition (AED) by heat shocking at 37^{o}C for 10 min. The crosses were kept at 25^{o}C and third instar larval wing discs were dissected, fixed and stained with DAPI for cell counting. The clones were marked with the absence of GFP expression. Clone areas were measured using the Histogram tool in Adobe Photoshop and presented as pixels.

I. Public data analysis

In this study we have utilized ChIPseq, ChIP-chip and microarray data from previously published articles and data deposited in public database. Genome-wide location data for GAF are from [32]. Enriched peaks were annotated to the nearest EnsEMBL [33] gene using Bioconductor package ChIPpeakAnno [34]. ChIPseq enriched location to nearest target genes were annotated similarly. However, location data extracted from modEncode database were confined to 3kb up- and down-stream from transcription start site (TSS) and database provided target annotation were considered. GAF targets from two different sources were uniquely combined. Gene expression microarray data of *rbf*, *wts* and *rbf wts* single and double mutants are from [6] (accession number GSE24978).

J. Gene ontology functional enrichment analysis

Functional annotation of target genes is based on Gene Ontology (GO) (Consortium, 2000; http://www.geneontology.org) as extracted from EnsEMBL [33]. Accordingly, all genes are classified into ontologies involved in Biological Process (BP). We have taken only the GO/pathway categories that have at least 10 genes annotated. We used Gitools software package for enrichment analysis and heatmap generation [35]. Resulting p-values were adjusted for multiple testing using the Benjamin and Hochberg's method of False Discovery Rate (FDR).

2.6. Literature cited

1. Pan D (2010) The hippo signaling pathway in development and cancer. Dev Cell 19: 491–505. doi:10.1016/j.devcel.2010.09.011.

2. Oh H, Irvine KD (2010) Yorkie: the final destination of Hippo signaling. Trends Cell Biol 20: 410–417. doi:10.1016/j.tcb.2010.04.005.

3. Peng HW, Slattery M, Mann RS (2009) Transcription factor choice in the Hippo signaling pathway: homothorax and yorkie regulation of the microRNA bantam in the progenitor domain of the Drosophila eye imaginal disc. Genes Dev 23: 2307–2319. doi:10.1101/gad.1820009.

4. Wu S, Liu Y, Zheng Y, Dong J, Pan D (2008) The TEAD/TEF family protein Scalloped mediates transcriptional output of the Hippo growth-regulatory pathway. Dev Cell 14: 388–398. doi:10.1016/j.devcel.2008.01.007.

5. Zhang L, Ren F, Zhang Q, Chen Y, Wang B, et al. (2008) The TEAD/TEF family of transcription factor Scalloped mediates Hippo signaling in organ size control. Dev Cell 14: 377–387. doi:10.1016/j.devcel.2008.01.006.

6. Nicolay BN, Bayarmagnai B, Islam ABMMK, Lopez-Bigas N, Frolov MV (2011) Cooperation between dE2F1 and Yki/Sd defines a distinct transcriptional program necessary to bypass cell cycle exit. Genes Dev 25: 323–335. doi:10.1101/gad.1999211.

7. Oh H, Irvine KD (2011) Cooperative regulation of growth by Yorkie and Mad through bantam. Dev Cell 20: 109–122. doi:10.1016/j.devcel.2010.12.002.

8. Richter C, Oktaba K, Steinmann J, Müller J, Knoblich JA (2011) The tumour suppressor L(3)mbt inhibits neuroepithelial proliferation and acts on insulator elements. Nat Cell Biol 13: 1029–1039. doi:10.1038/ncb2306.

9. Yang J, Corces VG (2011) Chromatin insulators: a role in nuclear organization and gene expression. Adv Cancer Res 110: 43–76. doi:10.1016/B978-0-12-386469-7.00003-7.

10. Lu J, Ruhf M-L, Perrimon N, Leder P (2007) A genome-wide RNA interference screen identifies putative chromatin regulators essential for E2F repression. Proc Natl Acad Sci USA 104: 9381–9386. doi:10.1073/pnas.0610279104.

11. Ambrus AM, Rasheva VI, Nicolay BN, Frolov MV (2009) Mosaic genetic screen for suppressors of the de2f1 mutant phenotype in Drosophila. Genetics 183: 79–92. doi:10.1534/genetics.109.104661.

12. Farkas G, Gausz J, Galloni M, Reuter G, Gyurkovics H, et al. (1994) The Trithorax-like gene encodes the Drosophila GAGA factor. Nature 371: 806–808. doi:10.1038/371806a0.

13. Adkins NL, Hagerman TA, Georgel P (2006) GAGA protein: a multi-faceted transcription factor. Biochem Cell Biol 84: 559–567. doi:10.1139/o06-062.

14. Lehmann M (2004) Anything else but GAGA: a nonhistone protein complex reshapes chromatin structure. Trends Genet 20: 15–22.

15. Morris EJ, Ji J-Y, Yang F, Di Stefano L, Herr A, et al. (2008) E2F1 represses beta-catenin transcription and is antagonized by both pRB and CDK8. Nature 455: 552–556. doi:10.1038/nature07310.

16. Hamaratoglu F, Gajewski K, Sansores-Garcia L, Morrison C, Tao C, et al. (2009) The Hippo tumor-suppressor pathway regulates apical-domain size in parallel to tissue growth. J Cell Sci 122: 2351–2359. doi:10.1242/jcs.046482.

17. Hamaratoglu F, Willecke M, Kango-Singh M, Nolo R, Hyun E, et al. (2006) The tumour-suppressor genes NF2/Merlin and Expanded act through Hippo signalling to regulate cell proliferation and apoptosis. Nat Cell Biol 8: 27–36. doi:10.1038/ncb1339.

18. Oh H, Irvine KD (2008) In vivo regulation of Yorkie phosphorylation and localization. Development 135: 1081–1088. doi:10.1242/dev.015255.

19. Oh H, Irvine KD (2009) In vivo analysis of Yorkie phosphorylation sites. Oncogene 28: 1916–1927. doi:10.1038/onc.2009.43.

20. Shopland LS, Hirayoshi K, Fernandes M, Lis JT (1995) HSF access to heat shock elements in vivo depends critically on promoter architecture defined by GAGA factor, TFIID, and RNA polymerase II binding sites. Genes Dev 9: 2756–2769.

21. Korenjak M, Taylor-Harding B, Binné UK, Satterlee JS, Stevaux O, et al. (2004) Native E2F/RBF complexes contain Myb-interacting proteins and repress transcription of developmentally controlled E2F target genes. Cell 119: 181–193. doi:10.1016/j.cell.2004.09.034.

22. Campbell S, Inamdar M, Rodrigues V, Raghavan V, Palazzolo M, et al. (1992) The scalloped gene encodes a novel, evolutionarily conserved transcription factor required for sensory organ differentiation in Drosophila. Genes Dev 6: 367–379.

23. Witcher M, Emerson BM (2009) Epigenetic silencing of the p16(INK4a) tumor suppressor is associated with loss of CTCF binding and a chromatin boundary. Mol Cell 34: 271–284. doi:10.1016/j.molcel.2009.04.001.

24. Nakayama T, Nishioka K, Dong Y-X, Shimojima T, Hirose S (2007) Drosophila GAGA factor directs histone H3.3 replacement that prevents the heterochromatin spreading. Genes Dev 21: 552–561. doi:10.1101/gad.1503407.

25. Wood AM, Van Bortle K, Ramos E, Takenaka N, Rohrbaugh M, et al. (2011) Regulation of chromatin organization and inducible gene expression by a Drosophila insulator. Mol Cell 44: 29–38. doi:10.1016/j.molcel.2011.07.035.

26. Petesch SJ, Lis JT (2008) Rapid, transcription-independent loss of nucleosomes over a large chromatin domain at Hsp70 loci. Cell 134: 74–84. doi:10.1016/j.cell.2008.05.029.

27. Lee H, Kraus KW, Wolfner MF, Lis JT (1992) DNA sequence requirements for generating paused polymerase at the start of hsp70. Genes Dev 6: 284–295.

28. Tsukiyama T, Wu C (1995) Purification and properties of an ATP-dependent nucleosome remodeling factor. Cell 83: 1011–1020.

29. Shimojima T, Okada M, Nakayama T, Ueda H, Okawa K, et al. (2003) Drosophila FACT contributes to Hox gene expression through physical and functional interactions with GAGA factor. Genes Dev 17: 1605–1616. doi:10.1101/gad.1086803.

30. Croston GE, Kerrigan LA, Lira LM, Marshak DR, Kadonaga JT (1991) Sequence-specific antirepression of histone H1-mediated inhibition of basal RNA polymerase II transcription. Science 251: 643–649.

31. Ross JF, Liu X, Dynlacht BD (1999) Mechanism of transcriptional repression of E2F by the retinoblastoma tumor suppressor protein. Mol Cell 3: 195–205.

32. Kharchenko PV, Alekseyenko AA, Schwartz YB, Minoda A, Riddle NC, et al. (2011) Comprehensive analysis of the chromatin landscape in Drosophila melanogaster. Nature 471: 480–485. doi:10.1038/nature09725.

33. Hubbard TJP, Aken BL, Beal K, Ballester B, Caccamo M, et al. (2007) Ensembl 2007. Nucleic Acids Res 35: D610–D617. doi:10.1093/nar/gkl996.

34. Zhu LJ, Gazin C, Lawson ND, Pagès H, Lin SM, et al. (2010) ChIPpeakAnno: a Bioconductor package to annotate ChIP-seq and ChIP-chip data. BMC Bioinformatics 11: 237. doi:10.1186/1471-2105-11-237.

35. Perez-Llamas C, Lopez-Bigas N (2011) Gitools: analysis and visualisation of genomic data using interactive heat-maps. PLoS ONE 6: e19541. doi:10.1371/journal.pone.0019541.

Part of this chapter used published work

3. Rb and Hippo pathways cooperate to maintain differentiation

3.1. Summary

The Rb pathway is inactivated in the majority of human cancers. This is commonly attributed to its key role in cell cycle regulation. Our previous work has unveiled a new role for the Rb pathway in *Drosophila*. In cooperation with the Hippo pathway, Rbf pathway maintains the identity of terminally differentiated cells. In the *Drosophila* retina, the photoreceptor clusters form during the third instar larval stage, express their markers and maintain the expression of their markers as they mature. Surprisingly, when both of these pathways are inactivated, via mutations in *rbf* and *wts*, we observed a widespread loss of differentiation markers. Importantly, this defect in differentiation is independent of the effect on cell proliferation. Here, we describe a novel lineage-tracing system we developed to mark photoreceptor cells. We showed that the cells that have lost the expression of their photoreceptor markers are not eliminated. Tissues with labeled cells were prepared into single cell suspensions and analyzed for transcriptional signature on the level of individual cells. Further analysis will determine the new identity of *rbf wts* double mutant cells.

3.2. Introduction

The larval eye imaginal disc is an excellent model for studying differentiation. Photoreceptor specifications occur in a highly organized fashion, and thus, even subtle perturbations of the differentiation pattern are easily visualized. The eye disc is divided into anterior and posterior compartments by the morphogenetic furrow. As the morphogenetic furrow moves from the posterior to anterior, the cells exit cell cycle and initiate their differentiation program. Therefore, the anterior compartment is composed of asynchronously dividing cells, while cells in the posterior are differentiating into photoreceptors (1,2). As photoreceptors differentiate, they form structures called ommatidial clusters. Each cluster consists of eight photoreceptor cells (R1-R8) that are recruited in a strict, sequential manner (3). The first photoreceptor to differentiate is R8, which expresses Sens. All mature photoreceptors (R1-R8) express the pan-neuronal marker ELAV (4). Surprisingly, when the Rbf and Hippo pathways were inactivated, via mutations in *rbf* and *wts*, we observed a widespread loss of differentiation markers, including Sens and ELAV (5).

To our knowledge, this is the first time such a profound differentiation defect had been reported in *Drosophila*. In mammalian systems, a number of studies came out underscoring the requirement of Rb for differentiation, including for osteogenic differentiation (6) and for the myogenic differentiation model (7). However, the most intriguing aspect of our phenotype is the fact that differentiation is initiated normally in our mutant tissues, but the differentiated state is not maintained over time.

The disappearance of photoreceptor-specific markers in the *rbf wts* double mutant tissue can be explained few different ways (Fig. 9A). First, these cells could simply be eliminated by apoptosis. This explanation is unlikely, however, because one of the classical target genes of the

Hippo pathway is *Drosophila inhibitor of apoptosis 1 (diap1)*, which protects cells from programmed cell death. Additionally, overexpression of the caspase inhibitor p35 in the *rbf wts* double mutant tissues failed to rescue the differentiation defect (5). In face of this compelling data, we still cannot formally rule out the possibility that these cells are eliminated via caspase-independent mechanisms.

If these cells are not eliminated in any way, but lost their photoreceptor identity, then they could have reverted to a progenitor-like state, thus dedifferentiated. This explanation is intriguing given that the most aggressive types of human tumors contain poorly differentiated cells. Considering the implication of both the Rb and Hippo pathways in human malignancies, it is tempting to postulate that they are also the guardians of the terminally differentiated state.

Another possible explanation is that the double mutant cells have transdifferentiated to another eye-specific cell type, such as the cone, bristle, or pigment cells. We observe the loss of photoreceptor markers during the third instar larval stage. Cone cell specification occurs during this stage, but the pigment and bristle cells differentiate later, during pupal development. Therefore, regarding transdifferentiation, a switch to a cone cell fate is more likely than to a pigment or a bristle cell.

Marker analysis done so far has major limitations and is an unfit tool for further analysis of the *rbf wts* mutant cells, which fail to maintain the expression of their markers. Unless these cells are labeled with a reporter, i.e. with a positive marker, we can never be certain that the right cell is being analyzed. Therefore, in order to reconcile among above possibilities, first, we have to clearly label the differentiated photoreceptors with a reporter, which is independent of the cell identity. We employed a combination of UAS/Gal4 (8) and the modified mFlp5/mFRT71 (9) systems to label photoreceptor cells with expression of the *lacZ* gene. *LacZ* expression is induced

in mature photoreceptors. However, its continued expression becomes independent of the developmental stage or cell identity, allowing us to follow the double mutant cells even after they lose the expression of their differentiation markers and subsequently, their identity.

Using this system, we can clearly visualize the β-Galactosidase (protein product of the *lacZ* gene)-positive double mutant cells, and have conclusively demonstrated that the double mutant cells persist in the eye discs, but lose their photoreceptor markers. Furthermore, single cell analysis will determine the new identity of these cells.

3.3. Results

A. Generation of a novel cell lineage tracing system

First and foremost, it was absolutely essential for us develop a lineage-tracing system for photoreceptors. Existing systems did not meet our requirements, for instance, by the presence of a classical Flp/FRT (10), which we would need to generate wts^{X1} mutant clones or the presence of an undesirable driver (11). We designed a system, by which all differentiated photoreceptor cells will also be marked by the expression of the *lacZ* gene (Fig. 9B). The *lacZ* gene will not be expressed unless the upstream transcriptional stop cassette is removed by Flp recombinase. Following this excision, *lacZ* will be brought under the regulation of the ubiquitous *actin5c* gene and its expression will be independent of the developmental stage or the identity of the cell. The expression of Flp recombinase is dependent on the photoreceptor-specific *elav* gene. Thereby, as a cell differentiates into a photoreceptor cell and expresses its marker *elav*, the downstream steps of the cell labeling system will take place and induce the expression of *lacZ*. Very importantly, if a cell were to lose its photoreceptor specific marker, ELAV, it would still retain the expression of β-Gal allowing us to follow these cells further.

The classical Flp/FRT system is routinely used for generating mosaic tissues via mitotic recombination. Therefore, we took advantage of the modified mFlp5/mFRT71 system for the excision of the transcriptional stop cassette (9). The transgenic fly stock containing the $act{\geq}stop{\geq}lacZ^{nls}$ (≥ indicates mFRT71 site) constuct was obtained from the laboratory of Dr. Barry Dickson. In order to utilize this reporter construct in a cell type-specific manner, we cloned the *mFlp5* gene downstream of *Upstream Regulating Sequences (UAS)* and generated *UAS-mFlp5* transgenic flies. These two constructs were recombined on a single chromosome

according to the crossing scheme in Fig. 10A. This set of transgenes will serve as the core of the cell labeling system and can be exploited for a variety of purposes in any cell type of interest.

In this case, the core labeling system will be expressed in the photoreceptor cells specifically. *Gal4* transactivator under the regulation of the photoreceptor-specific *elav* gene was recombined with the chromosome harboring the null wts^{X1} mutation on chromosome III (Fig. 10A). Then, all transgenes assembled on separate chromosomes were combined in a single animal. This way, the stock is ready to be crossed to flies carrying a mutation in the *rbf* gene and containing the components required for generating the mosaic tissue.

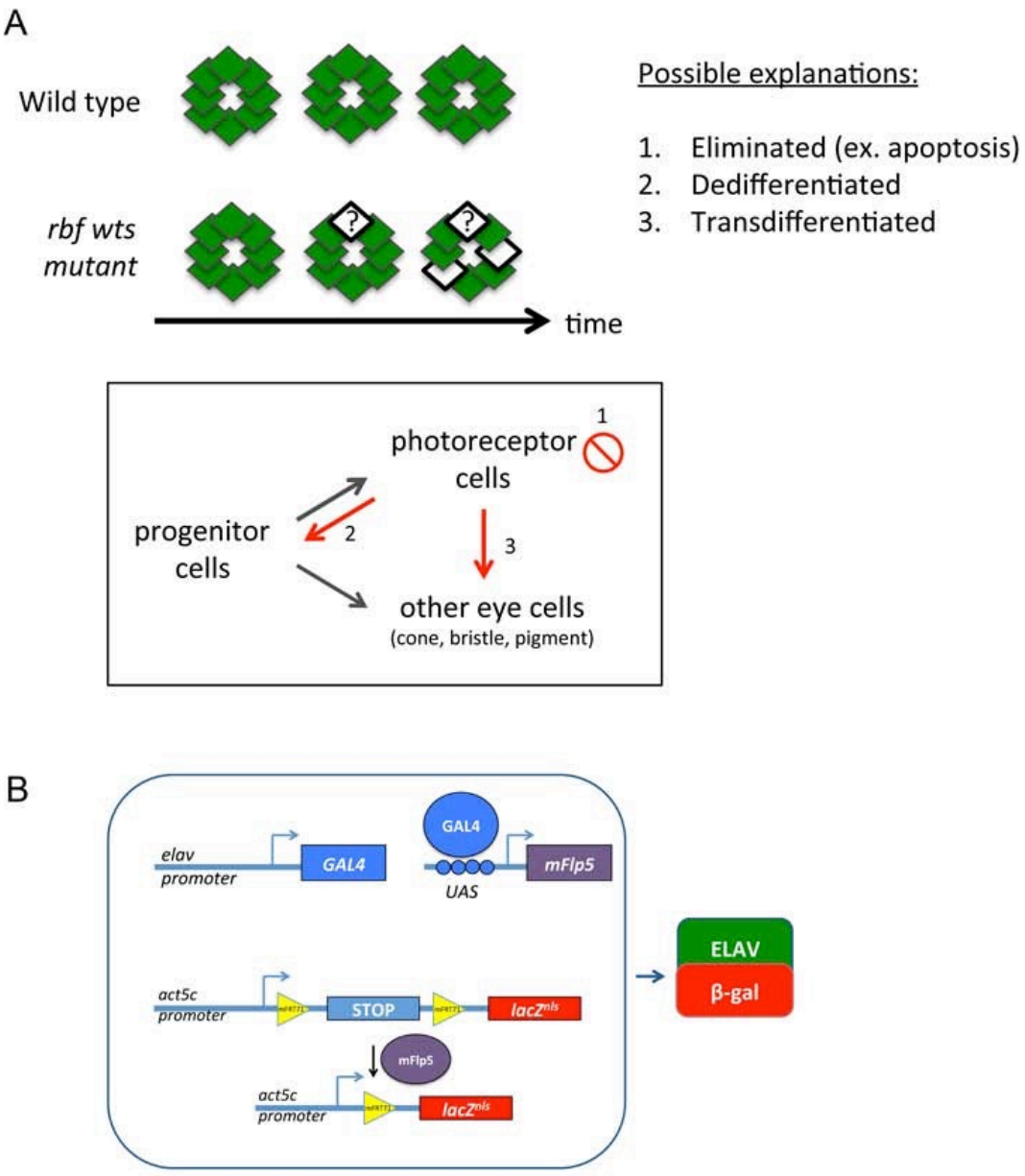

Figure 9. Photoreceptor cell lineage tracing system.

(A) The schematic representation of the *rbf wts* mutant phenotype. One ommatidial cluster is represented by green diamonds. The white diamonds are photoreceptors that lost the expression of their markers. The model of possible explanations for the loss or markers.
(B) The schematic design for photoreceptor cell lineage tracing with the expression of *lacZ.*

B. Validating the cell lineage-tracing system

Each step of generating the system was functionally validated *in vivo*. To check recombination on the second chromosome, we drove the expression of *UAS-mFlp5, act≥stop≥lacZ*^{nls} in imaginal discs and performed immunofluorescence for β-Gal. In the eye imaginal disc, we used the *GMR-Gal4* driver, which is a string driver and expresses genes in all differentiated eye cells (Fig. 10B). In the negative control wild type *Canton S* pupal eye discs, ELAV marks all photoreceptors, however there is no β-Gal staining, as expected. β-Gal expression is detected in all eye cells when *GMR* drove *UAS-mFlp5, act≥stop≥lacZ*^{nls}. To confirm this result, we used a different driver for the wing disc. *ptc-Gal4* is expressed in a stripe along the anterior/posterior boundary as shown in a wild type *Canton S* wing disc (Fig. 10C). β-Gal protein is detected in the precise stripe, identical to the wild type Ptc expression pattern.

There are two elements on the third chromosome. First, the *elav-Gal4* transgene was tested by crossing it to *UAS-GFP*. ELAV protein is detected in the photoreceptor cells in the posterior of the eye disc. GFP driven by GAL4 can also be seen in the posterior (Fig. 10D). This expression is delayed, but it is consistent with the strength of the driver. The second element is the *82BFRT wts*^{X1}, which are required for generating the mutant clones harboring a null mutation in the *wts* gene. We crossed the stock to *ey-Flp; 82BFRT GFP* to generate clones in the eye imaginal disc and mark clones with presence or absence of GFP. This cross yielded clones, which confirms the presence of the *82BFRT* element required for mitotic recombination. We also observed that the GFP-negative mutant tissue was overgrown compared to the GFP-positive wild type clone, indicating that we recovered the *wts*^{X1} null allele (Fig. 10E).

Lastly, these two chromosomes were combined in a single animal. All individual elements were tested again as described above (data not shown).

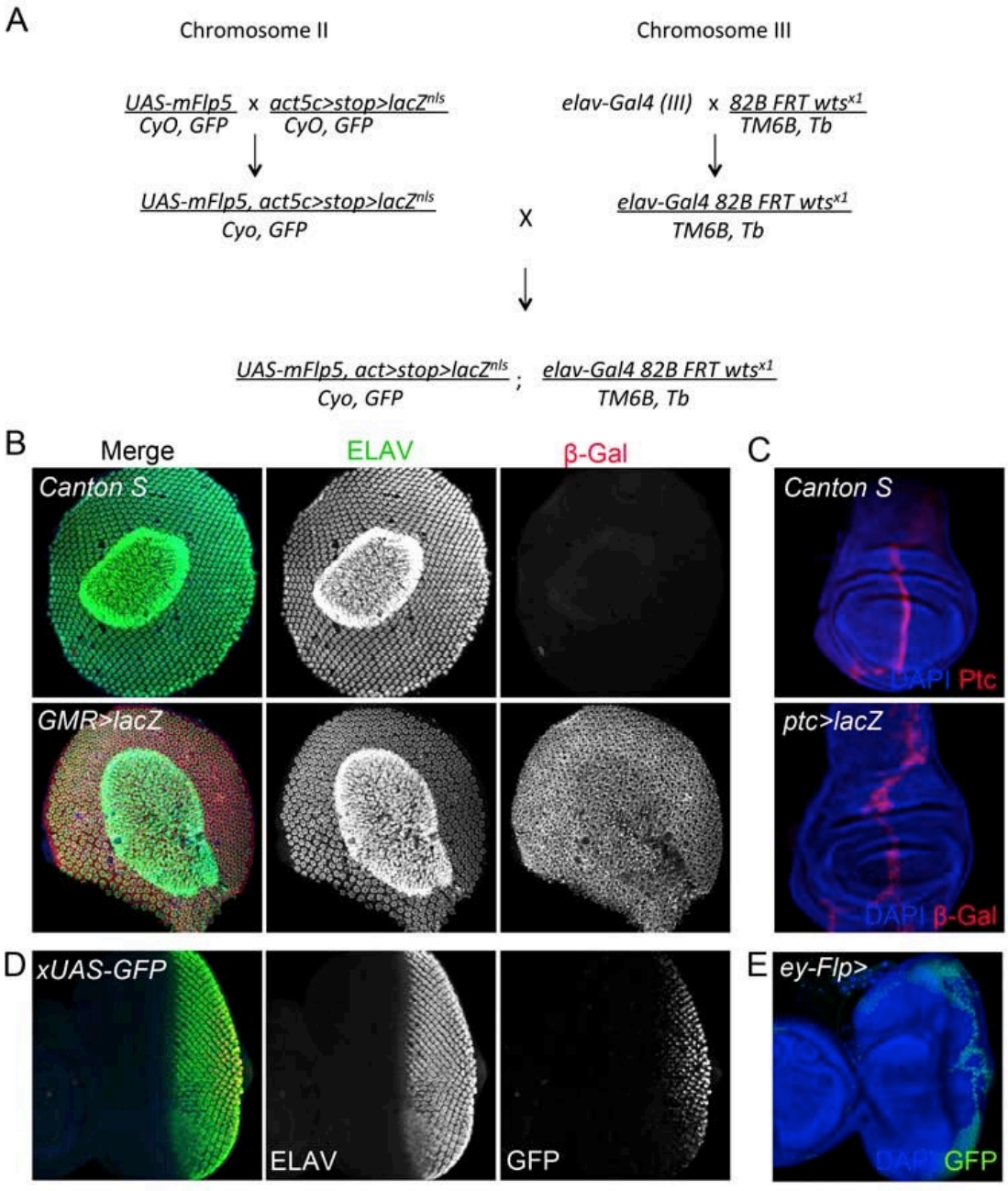

Figure 10. Crossing scheme and validation of the lineage-tracing system.

(A) Crossing scheme for assembling the components of the cell labeling system.
(B, C) Validation of transgenes on chromosome II.
(B) 48hr APF pupal eye disc of wild type *Canton S* flies show ommatidial clusters stained with ELAV (green) and no staining for β-Gal (red). *GMR>mFlp5, act5c≥stop≥lacZ* eye disc shows β-Gal in all cells of the eye disc.

(C) Ptc protein expression pattern in a wild type *Canton S* wing disc. *ptc-Gal4* driven *UAS-mFlp5, act5c≥stop≥lacZ* β-Gal protein pattern. DAPI (blue), β-Gal (red).
(D, E) Validation of transgenes on chromosome III.
(D) *elav-Gal4 82BFRT wts*^{X1} crossed to *UAS-GFP* shows GFP protein expression in ELAV-expression pattern at the posterior of the eye disc. ELAV (green), GFP (red) in the merged image.
(E) *ey-Flp; 82BFRT GFP* crossed to *elav-Gal4 82BFRT wts*^{X1}. Wild type clones are marked by GFP (green) and the mutant clones are marked by the absence of GFP. DAPI marks nuclei (blue).

C. Assessing the efficiency of labeling

After the final stock was made, we tested the efficiency of the system in labeling photoreceptors. Because the system consists of multiple steps, we reasoned that it might require a substantial amount of time. Consistent with our prediction, β-Gal could not be detected at the third instar larval stage (Fig. 11A). However, we could clearly detect its expression at the mid-pupal stage at 48hr after pupa formation (APF) (Fig. 11A).

In theory, every single cell expressing ELAV should also express β-Gal, according to our design. In practice, that is not the case. We observe photoreceptor clusters containing varying numbers of β-Gal-positive cells (Fig. 11B). Quantification determined that on average, there are two β-Gal-positive cells per ommatidial cluster, or 28% efficiency of labeling. Most importantly, every β-Gal-positive cell was also positive for ELAV, indicating that a 100% of labeled cells are specifically photoreceptors.

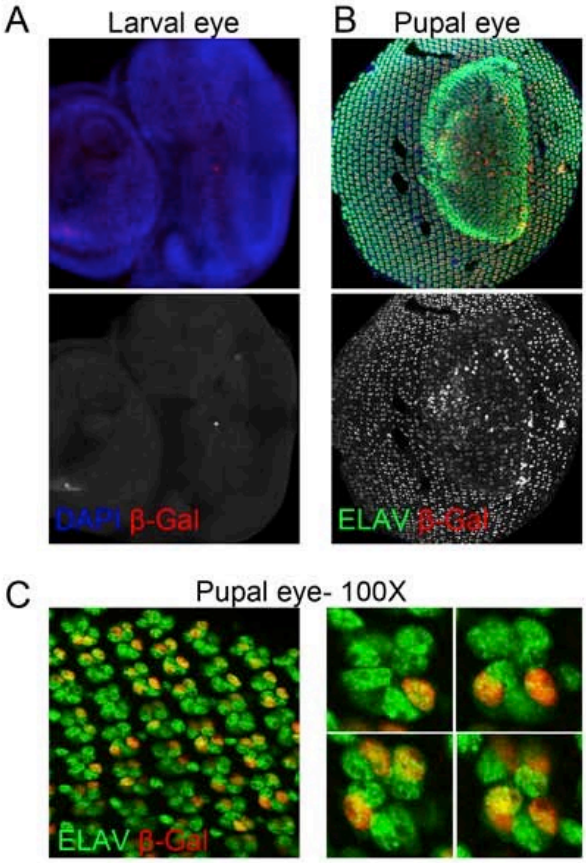

Figure 11. Labeling efficiency of the lineage-tracing system.

(A) Third instar larval eye disc of *UAS-mFlp5, act5c≥stop≥lacZ; elav-Gal4 82BFRT wts*^{X1} stock. No β-Gal (red) is detected, DAPI (blue).
(B) 48hr APF pupal eye disc of the same stock. ELAV (green) marks photoreceptor cells. β-Gal (red) is detected in photoreceptor cells.
(C) 100X zoomed-in image of 48hr APF pupal eye disc. ELAV (green) and β-Gal (red) co-localize in photoreceptor cells.

D. *rbf wts* double mutant cells are not eliminated

With the cell labeling system in place, now we are able to analyze the *rbf wts* mutant cells by labeling the photoreceptor cells in the background of the *rbf wts* mutation. We looked at the mid-pupal eye discs at approximately 48hr APF, and stained for the photoreceptor marker ELAV and β-Gal (Fig. 12A, whole disc). From the whole disc we can clearly see the GFP-negative mutant clones where ELAV expression is disorganized and disrupted. The photoreceptor reporter β-Gal expression is scattered throughout the tissue.

In Fig. 12B, we zoom into a portion of the pupal disc. In the wild type clone, marked by GFP, all β-Gal-positive cells also express ELAV, consistent with our validation results (magenta arrows). We also observe the same combination in the GFP-negative double mutant tissue, as not all mutant photoreceptors are losing their markers (5). As expected, we see a number of ELAV-positive photoreceptor cells that weren't labeled with β-Gal in both wild type and mutant clones (white arrows).

Upon further scrutiny, the photoreceptor cells expressing β-Gal, which is dependent on the expression of the *elav* gene, were missing ELAV protein. Strikingly, this β-Gal positive/ELAV negative combination is observed only in the *rbf wts* double mutant tissue. This means that the double mutant cells expressed *elav* gene, then consequently the *lacZ* gene, differentiated into photoreceptors and somehow through the course of development failed to maintain the expression of the *elav* gene and the ELAV protein. This result is a proof that *rbf wts* double mutant cells lose their differentiation marker, but are not eliminated by apoptosis or otherwise.

Importantly, this defect is not a consequence of overproliferation. Overexpression of the constitutively active yki^{S168A} is not sufficient to induce loss of photoreceptors (Fig. 13A). Here,

yki^{S168A} expression was induced much earlier in development with a heat shock driver. Even though *yki*^{S168A} promotes over-proliferation and tissue overgrowth, in the *rbf* mutant background differentiated photoreceptor clusters retain the expression of Sens (red) and ELAV (blue) (Fig. 13A). This result is in full agreement with our previous finding of *yki*^{S168A} overexpression in postmitotic photoreceptor cells with the *GMR* driver.

In order to determine whether this phenotype is merely a consequence of inactivating two tumor suppressors, we analyzed *rbf tsc* double mutant tissue. *tsc* inactivation on its own results in cell growth and mild acceleration in cell cycle progression, but terminal differentiation occurs normally (12,13). In *rbf tsc* double mutant tissue, differentiation was unaffected as indicated by the unperturbed pattern of Sens positive cells (Fig. 13B). Based on these observations and other experimental evidence presented by our lab, committed photoreceptor cells are losing their differentiation markers upon simultaneous inactivation of RBF and Hippo pathways specifically.

From our three explanations for the disappearance of the photoreceptor markers in *rbf wts* mutant cells (Fig. 9A), we can reject the possibility that these cells are eliminated.

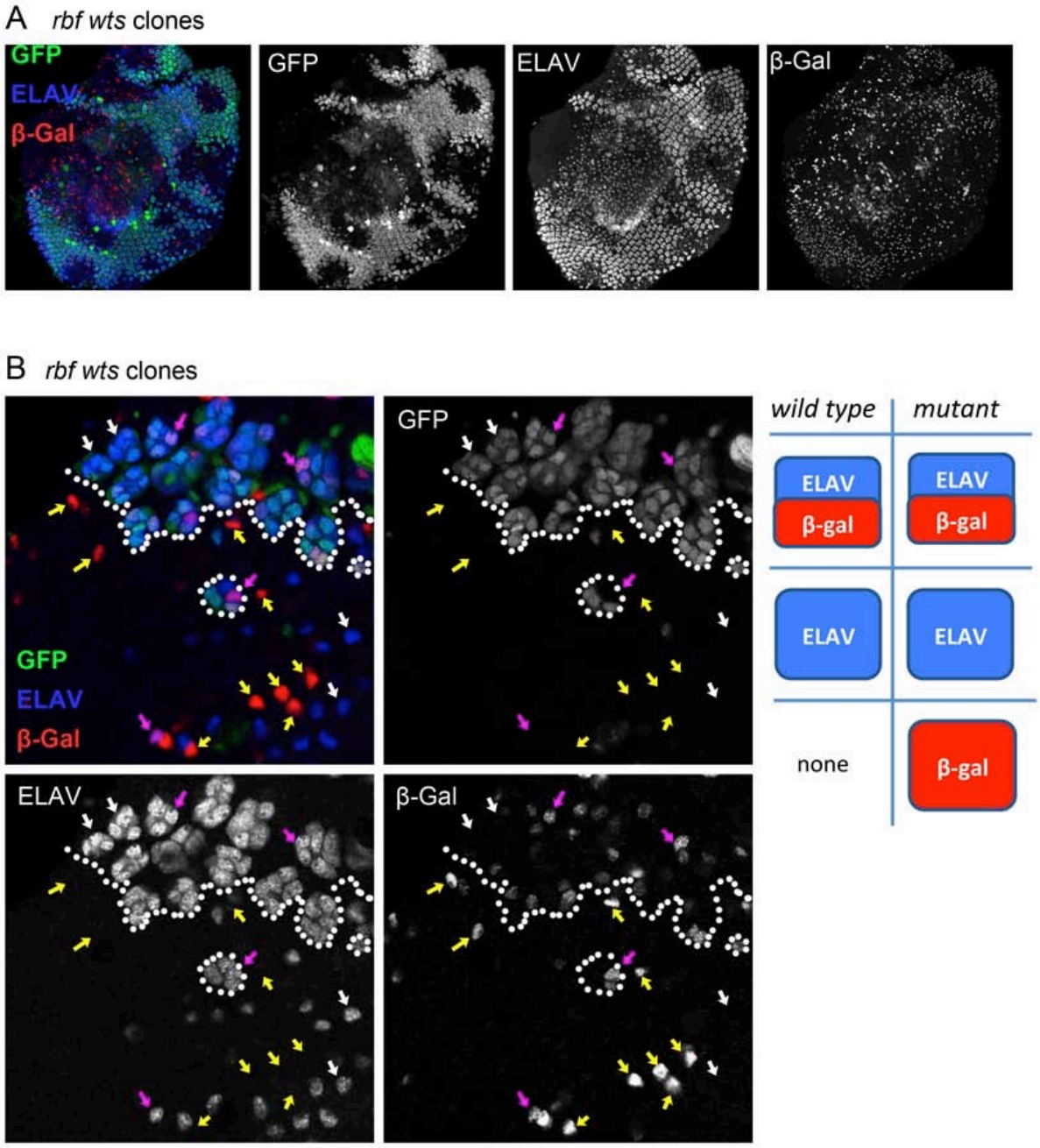

Figure 12. rbf wts mutant photoreceptor cells are not eliminated.

(A) 48hr APF pupal eye disc. *rbf wts* mutant clones are marked by the absence of GFP (green), photoreceptor cells are stained for ELAV (blue) and β-Gal (red).
(B) 100X zoomed-in image. The dotted line marks the border between the wild type and mutant clones. White arrows point at ELAV-positive photoreceptor that were not labeled with β-Gal. Magenta arrows point at photoreceptor cells that are positive for both ELAV and β-Gal. Yellow arrows point at β-Gal-positive photoreceptors which have lost ELAV. The chart on the right shows the distribution of the label combinations in each genotype.

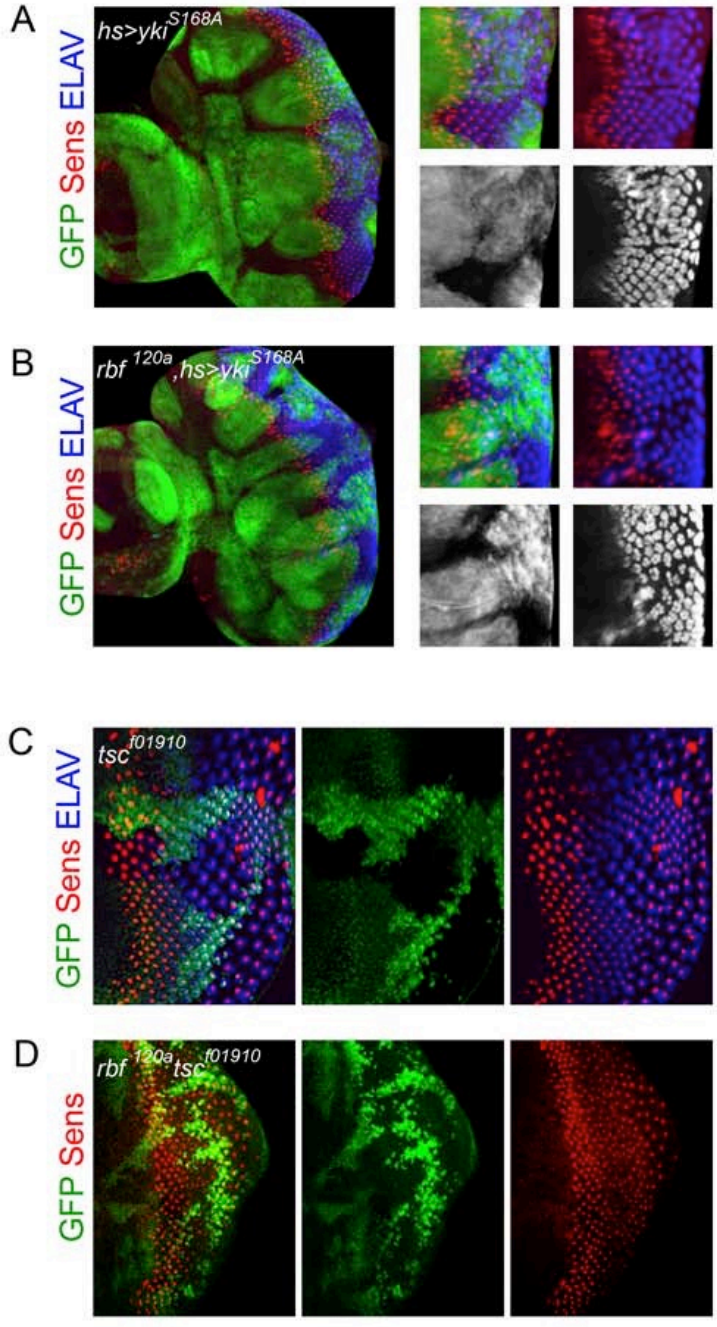

Figure 13. Loss of photoreceptor phenotype is specific to mutations in *rbf* and *wts*.

Third instar eye imaginal discs stained with differentiation markers, Sens (red) and ELAV (blue). (A) Heat shock-induced yki^{S168A} overexpressing clones marked by GFP. *Right,* zoomed-in images of separate channels reveal that in both wild type (GFP-negative) and > yki^{S168A} expressing clones (GFP-positive) display normal distribution of Sens and ELAV.
(B) Heat shock-induced yki^{S168A} overexpressing clones marked by GFP in the background of rbf^{l20a} mutant. The hyperactive yki^{S168A} is not sufficient to trigger loss of Sens and ELAV expression even when the RBF pathway is deregulated.

(C-D) Mutation of the tumor suppressor gene *tsc* alone (C) or in conjunction with *rbf* is not sufficient to disrupt the expression of Sens and ELAV. GFP marks wild type clone, lack of GFP marks the mutant clone.

E. Determining the new identity of the *rbf wts* cells

With this labeling system, we can now move forward in efforts to determine the new identity adopted by the *rbf wts* cells. The heterogeneous nature of the tissue we work with, in terms of both cell type and genotype, make it difficult to study bulk samples. The surrounding tissue can easily mask the effects in the *rbf wts* cells. Therefore, we decided to characterize them on the level of single cells. Fluidigm Corporation has developed an integrated fluidic circuit technology to distribute single cells into separate wells. Each cell can individually be assayed for gene expression. To our knowledge, this technology hasn't been exploited for single cell studies from *Drosophila* tissues. It has, however, been used to successfully differentiate all cell types in a mouse lung (14) and define sub-states of pluripotency (15).

We optimized the conditions for imaginal disc dissociation, single cell capture and gene expression on wild type tissues expressing the photoreceptor cell labeling system. Third instar larval eye discs were severed from the antennal disc and dissociated into a single cell suspension in a Trypsin/PBS solution (Fig. 14A). Recovered single cells were re-suspended in BSA/PBS solution and separated into individual wells with the C1 Single-Cell Auto Prep System (Fig. 14A, right panels). mRNA and cDNA are generated in the same run by the C1 Single-Cell Auto Prep System. Then we measured expression levels of select genes with Biomark HD single cell qPCR machine. We could measure the reference gene *rp49* in all cells assayed (Fig. 14B). These cells segregated by their expression of *lacZ,* which is induced only in the photoreceptor cells. This shows that despite the protein β-Gal not being detected at the third instar larval stage, the gene is clearly expressed. The *lacZ* mRNA expression can be used to distinguish the labeled photoreceptors from other cells of the eye imaginal disc. Now we have the genetic tool to

identify photoreceptor cells as well as the methodology to accurately assay their gene expression pattern.

In order to determine whether the *rbf wts* mutant cells have dedifferentiated or transdifferentiated, we must compare the transcriptional signature of these cells to the signatures of progenitors and other eye cell types. Except for a handful of cell type specific markers, to date, there are no available transcriptional data of purified cell populations. The only resource is the microarray analysis done in the larval eye disc, where progenitor (GMR-) vs differentiated (GMR+) cell populations were sorted and assayed (16). This data gave an insight into the transcriptional differences between progenitor cells and differentiating posterior cells, which include photoreceptors and all interommatidial cells that are poised to be specified. The data still is an average of a heterogeneous population of cells. Therefore, we utilized the single cell analysis approach. This method will not only characterize the *rbf wts* mutant cells, but also give wild type cell fate- specific transcriptional signatures and identify novel markers.

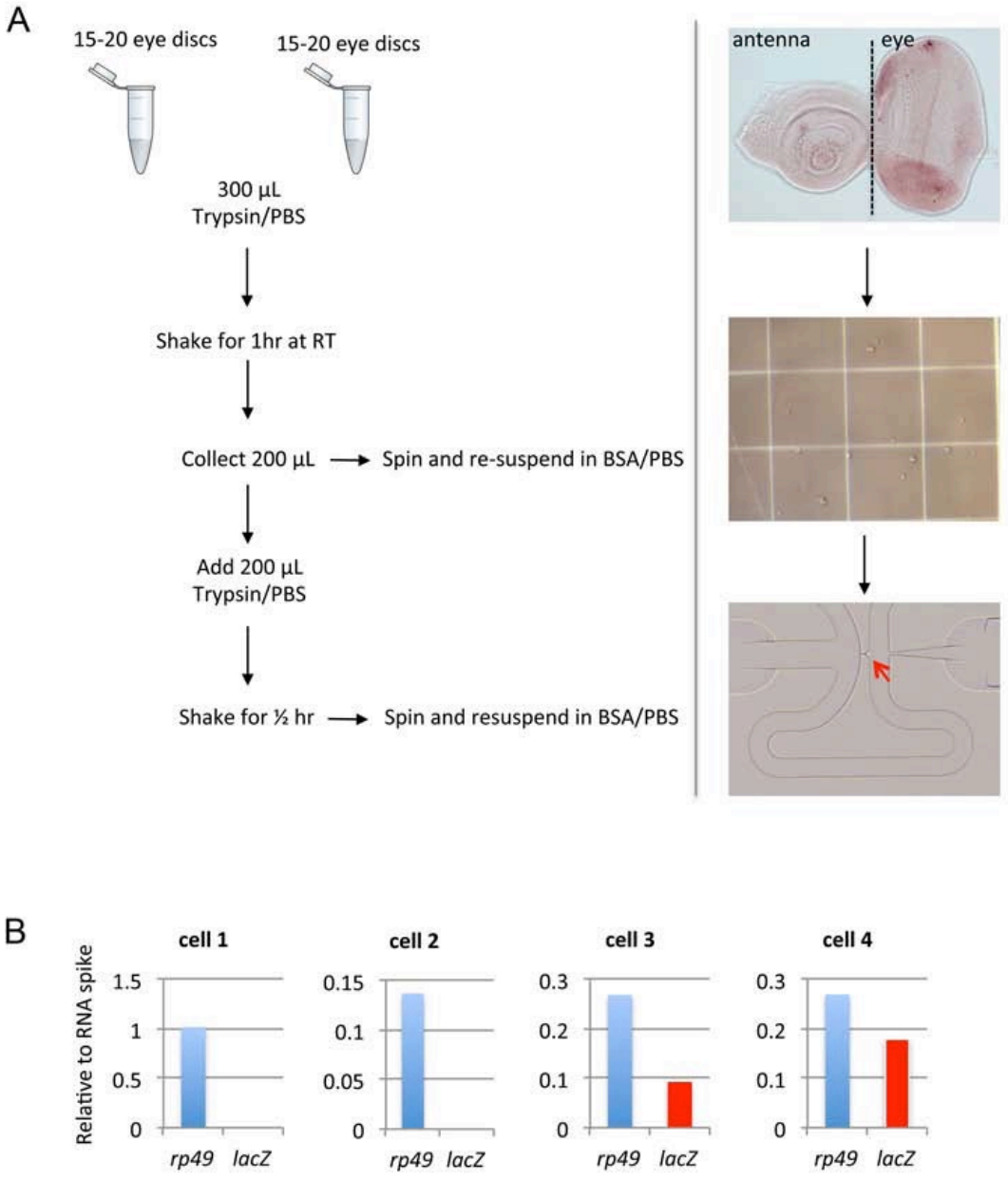

Figure 14. Single cell analysis.

(A) *Left,* tissue dissociation procedure. *Right,* images for the third instar larval eye disc, which was separated from the antennal disc, dissociated into a single cell suspension and captured in individual wells (red arrow).
(B) Gene expression of four representative captured single cells from *UAS-mFlp5, act5c≥stop≥lacZ; elav-Gal4 82BFRT wts*^{X1} stock. *rp49* is a reference gene. Cells can be segregated by the expression of the photoreceptor- specific *lacZ* gene.

3.4. Discussion

It is widely believed that in multicellular organisms terminal differentiation is accompanied by the loss of cellular plasticity. This notion of irreversibility has been challenged with mounting evidence, including nuclear transfer experiments (17) and most powerfully, by the iPS technology (18). During adulthood, when organs experience mechanical damage, they initiate many processes to repair the damaged tissue. These processes include adult stem cell activation, expansion of the existing cells, dedifferentiation or even transdifferentiation (reviewed in (19)). These data reveal the remarkable plasticity of terminally differentiated cells.

Our work has uncovered a novel setting where the terminally differentiated state has been compromised by inactivation of the RBF and Hippo tumor suppressor pathways (5). In these mutant cells, the photoreceptor cells differentiate and form normally, but over time fail to maintain the expression of their photoreceptor-specific markers. Here, we have for the first time visualized the *rbf wts* cells and completed the groundwork for further characterization by creating the novel photoreceptor cell lineage tracing system.

Out of the three plausible explanations we proposed, we rejected the possibility that the *rbf wts* cells, which have lost the expression of their markers, have simply been eliminated. We conclusively demonstrated the persistence of once differentiated, β-Gal expressing cells that failed to maintain the expression of ELAV (Fig. 12B). Notably, these cells are found only in the *rbf wts* mutant clones, confirming the requirement for both the Rb and Hippo pathways to maintain their differentiated state. Additionally, the loss-of-markers phenotype is much more severe than presented as we are likely to be underestimating the frequency of these events considering the 28% efficiency of cell labeling events (Fig. 11).

Determining the new fate of the *rbf wts* mutant cells is particularly exciting in light of new emerging roles for both the Rb and the Hippo pathways. In a murine model of liver development, it has been shown that hepatocytes dedifferentiate to progenitor-like cells following acute inactivation of the Hippo pathway. These dedifferentiated cells were capable of giving rise to mature hepatocytes only if the proper function of the pathway was restored (20). The pRb protein has been shown to promote differentiation by interacting with cell type-specific factors, as in osteogenic program (6), and more recently, by de-repressing genes required for mitochondrial activity (21).

With a change in cell fate comes a change in cell morphology, shape, size and function. Particularly, if we are considering the switch from a rod-shaped photoreceptor cell with its elongated rhabdomere and extending axonal projections to a progenitor cell, for instance, one can imagine a great deal of tissue reorganization to accommodate such a dramatic transformation. However, with its implications in sensing intra- and extra-cellular mechanical tensions, cell geometry and cell-cell contact, the Hippo pathway is one of the best candidates fit for the job (22).

In order to determine the precise roles of the Rb and Hippo pathways in maintenance of differentiation, especially in complex and heterogeneous tissues, such as the eye imaginal discs, it is of utmost importance to accurately identify the cells of interest. Therefore, we placed a tremendous amount of importance in developing the lineage-tracing system. It is critical to note that the lineage-tracing system is designed to be highly flexible. The core construct *UAS-mFlp5, act5c≥stop≥lacZ* can be driven in any cell- or tissue-specific manner. Additionally, the use of the modified mFlp5/mFRT71 system allows for combination of this cassette with stocks carrying the commonly used classical Flp/FRT system with no cross reactivity. We have generated an

alternative version by replacing the *lacZ* gene with GFP. This will permit following the labeled cells *in vivo*, live imaging and fluorescence-activated cell sorting (FACS) to enrich for certain cell populations. This system proves to be a valuable tool and contributes to the rich variety of genetic tools available in *Drosophila.*

With the rising awareness of cellular heterogeneity even among the cells of the same origin, more effort has been placed on increasing the precision and accuracy of our measurements. One of the state of the art methods is the integrated fluidic circuit technology developed by the Fluidigm Corporation. This system separates single cells and performs lysis, mRNA and cDNA generation of individual cells in nanoliter volumes of reactions. This method has been successfully used to segregate all cell types of a mouse distal lung (14). To our knowledge, this technology has not been exploited in *Drosophila.* We are utilizing this technology to determine cell type-specific transcriptional programs on a single cell level and identify the new fate the *rbf wts* mutant cells may have adopted.

3.5. Materials and methods

A. Fly stocks

All fly stocks were kept at 25°C on standard cornmeal agar food.

The following fly stocks were generated:
UAS-mFlp5 (II)
UAS-mFlp5, act5c≥stop≥lacZ
UAS-mFlp5, act5c≥stop≥lacZ; elav-Gal4 82BFRT wts^{X1}

Additional fly stocks used:
GMR-Gal4 (II)
elav-Gal4 (III)
ptc-Gal4 (II)
rbf^{120a}*, ey-Flp; 82BFRT GFP*
82BFRT wts^{X1}

B. Cloning- UAS-mFlp5

ey-mFlp5 construct was a generous gift from the Salecker lab. *mFlp5* was digested with BglII and XbaI and inserted into pUAST transformation vector. The embryo injections were done by BestGene Inc. (Chino Hills, CA). Ten transgenic animals with germline insertions were obtained, the insertions were mapped and one line with the insertion on the second chromosome was tested and used for further studies.

C. Immunofluorescence

Antibodies used were mouse anti-Ptc (DSHB, 1:50), rat anti-ELAV (DSHB, 1:150), mouse anti-β-gal (DSHB, 1:200), Cy3- and Cy5-conjugated secondary antibodies (Jackson ImmunoLaboratories, 1:200). The cells were also stained with DAPI (Sigma). Larval and pupal tissues were fixed in 4% formaldehyde for 30 min on ice, washed in phosphate-buffered saline and 0.3% Triton X-100 (PBST) and incubated with the primary antibodies overnight in PBST

and 10% normal donkey serum. The samples were incubated with the secondary antibodies for 1hr at RT at the concentration of 1:200. The imaginal discs were then washed in PBST and stored in glycerol with propyl gallate anti-fade reagent. The images were captured using the Zeiss LSM700 confocal microscope.

D. Single Cell Analysis- tissue dissociation

Third instar eye imaginal discs were dissected and detached from the antennal portion in Schneider medium. The discs were allowed to sink to the bottom of the tube. The Schneider medium was replaced with 300 ul of 10X Trypsin (Sigma-Aldrich) in PBS solution. The tubes were placed on conventional tabletop shaker for 1 hour at room temperature with occasional mild vortexing for 5-10 sec. After 1 hour, the clumps were allowed to sink to the bottom of the tube for 5 min and the top portion containing dissociated single cells was transferred to a new tube. In the meantime, the 200 ul of fresh Trypsin/PBS solution was replaced in the tube with tissue chunks and placed on the shaker for additional 30 min. The collected single cell suspensions were spun at 2000 rpm at 4^{o}C for 5min and resuspended in 1% BSA/1X PBS solution. The cells were filtered through a cell strainer and quantified using a hemocytometer. Trypan blue staining was used to assess percent viability.

E. Single Cell Analysis- C1 capture, BioMark HD qPCR

Single cell suspension was separated on C1 Auto-Prep system into individual wells. The cells were lysed and the cDNA was generated in the same system. Primers at low concentration were added for pre-amplification step. Pre-amplified amplicons were detected for gene expression

measured Biomark HD qPCR machine. All experiments were carried out according to the protocols recommended by Fluidigm corporation.

3.6. Literature cited

1. Kumar JP. Building an ommatidium one cell at a time. Singh A, Irvine KD, editors. Dev Dyn. 2011 Dec 15;241(1):136–49.

2. Carthew RW. Pattern formation in the Drosophila eye. Current Opinion in Genetics & Development. 2007 Aug;17(4):309–13.

3. Freeman M. Reiterative use of the EGF receptor triggers differentiation of all cell types in the Drosophila eye. Cell. 1996 Nov 15;87(4):651–60.

4. Robinow S, White K. The locus elav of Drosophila melanogaster is expressed in neurons at all developmental stages. Developmental Biology. 1988 Apr;126(2):294–303.

5. Nicolay BN, Bayarmagnai B, Moon NS, Benevolenskaya EV, Frolov MV. Combined inactivation of pRB and hippo pathways induces dedifferentiation in the Drosophila retina. PLoS Genet. 2010 Apr;6(4):e1000918.

6. Thomas DM. Terminal osteoblast differentiation, mediated by runx2 and p27KIP1, is disrupted in osteosarcoma. The Journal of Cell Biology. 2004 Dec 6;167(5):925–34.

7. Benevolenskaya EV, Murray HL, Branton P, Young RA, Kaelin WG. Binding of pRB to the PHD protein RBP2 promotes cellular differentiation. Molecular Cell. Elsevier; 2005 Jun 10;18(6):623–35.

8. Brand AH, Perrimon N. Targeted gene expression as a means of altering cell fates and generating dominant phenotypes. Development. 1993 Jun;118(2):401–15.

9. Hadjieconomou D, Rotkopf S, Alexandre C, Bell DM, Dickson BJ, Salecker I. Flybow: genetic multicolor cell labeling for neural circuit analysis in Drosophila melanogaster. Nat Meth. 2011 Feb 6;8(3):260–6.

10. Golic KG, Lindquist S. The FLP recombinase of yeast catalyzes site-specific recombination in the Drosophila genome. Cell. 1989 Nov 3;59(3):499–509.

11. del Valle Rodríguez A, Didiano D, Desplan C. Power tools for gene expression and clonal analysis in Drosophila. Nat Meth. 2011 Dec 28;9(1):47–55.

12. Tapon N, Ito N, Dickson BJ, Treisman JE, Hariharan IK. The Drosophila tuberous sclerosis complex gene homologs restrict cell growth and cell proliferation. Cell. 2001 May 4;105(3):345–55.

13. Potter CJ, Huang H, Xu T. Drosophila Tsc1 functions with Tsc2 to antagonize insulin signaling in regulating cell growth, cell proliferation, and organ size. Cell. 2001 May 4;105(3):357–68.

14. Treutlein B, Brownfield DG, Wu AR, Neff NF, Mantalas GL, Espinoza FH, et al. Reconstructing lineage hierarchies of the distal lung epithelium using single-cell RNA-

seq. Nature. Nature Publishing Group; 2014 May 6;509(7500):371–5.

15. Hough SR, Thornton M, Mason E, Mar JC, Wells CA, Pera MF. Single-Cell Gene Expression Profiles Define Self-Renewing, Pluripotent, and Lineage Primed States of Human Pluripotent Stem Cells. Stem Cell Reports. The Authors; 2014 Jun 3;2(6):881–95.

16. Jasper H, Benes V, Atzberger A, Sauer S, Ansorge W, Bohmann D. A genomic switch at the transition from cell proliferation to terminal differentiation in the Drosophila eye. Developmental Cell. 2002 Oct;3(4):511–21.

17. GURDON JB. The developmental capacity of nuclei taken from intestinal epithelium cells of feeding tadpoles. J Embryol Exp Morphol. 1962 Dec;10:622–40.

18. Takahashi K, Yamanaka S. Induction of Pluripotent Stem Cells from Mouse Embryonic and Adult Fibroblast Cultures by Defined Factors. Cell. 2006 Aug;126(4):663–76.

19. Jessen KR, Mirsky R, Arthur-Farraj P. The Role of Cell Plasticity in Tissue Repair: Adaptive Cellular Reprogramming. Developmental Cell. Elsevier Inc; 2015 Sep 28;34(6):613–20.

20. Yimlamai D, Christodoulou C, Galli GG, Yanger K, Pepe-Mooney B, Gurung B, et al. Hippo Pathway Activity Influences Liver Cell Fate. Cell. Elsevier Inc; 2014 Jun 5;157(6):1324–38.

21. Váraljai R, Islam ABMMK, Beshiri ML, Rehman J, Lopez-Bigas N, Benevolenskaya EV. Increased mitochondrial function downstream from KDM5A histone demethylase rescues differentiation in pRB-deficient cells. Genes Dev. 2015 Sep 4;29(17):1817–34.

22. Low BC, Pan CQ, Shivashankar GV, Bershadsky A, Sudol M, Sheetz M. YAP/TAZ as mechanosensors and mechanotransducers in regulating organ size and tumor growth. FEBS Letters. Federation of European Biochemical Societies; 2014 Aug 19;588(16):2663–70.

4. Therapeutic activation of pRb by small molecule inhibitor PD0332991 leads to elevated mitochondrial activity

4.1. Summary

The Rb pathway is a key regulator of the cell cycle. Inactivation of this pathway is considered to be an obligatory step for cancer progression. In the clinic, Rb status is an important determinant of cancer progression, disease outcome and prognosis. Therapeutic activation of the Rb protein with the Cyclin D/CDK4 inhibitor PD0332991 (Palbociclib) robustly arrests cells in G1. Additionally, this treatment upregulates the expression of mitochondria-associated genes and as a result, mitochondrial activity. This activity is required for apoptosis in response to cytotoxic agents. However, cell lines exhibit varying levels of sensitivity to genotoxic agents following PD0332991 treatment. The normal breast tissue cells MCF10A and the cancer cell line MCF7 can be sensitized to doxorubicin-induced apoptosis when pre-treated with PD0332991. In contrast, the more aggressive MDA-MB-231 cancer cells exhibited higher resistance to cell death, despite the increase in mitochondrial activity following PD0332991 treatment. In the clinical setting, these factors must be taken into account when treatments are designed for individual patients.

4.2. Introduction

In light of increasing evidence of the Rb and Hippo pathways interacting, we sought to identify more points of crosstalk between these two pathways. A hint came from a study where overexpression of the *Drosophila yki* in wing discs or mammalian *YAP2* in human breast cancer cell lines lead to enhanced mitochondrial mass, elongated and enlarged mitochondria (1). Similarly, Rb/E2f axis has been linked to mitochondrial activity (2). Our lab showed that the Rb pathway directly regulates mitochondria-associated genes in flies and the human osteosarcoma cell line *SAOS2*. Disruption of the Rb pathway leads to punctate mitochondrial morphology and reduced activity (3). Therefore, we asked whether Rb and Hippo pathways cooperate to regulate mitochondrial function.

Mitochondria are highly dynamic organelles that are major suppliers of cellular energy, which they provide in the form of ATP via oxidative phosphorylation. Mitochondria also play important roles in various biochemical pathways, such as The Citric Acid Cycle (TCA), β-oxidation of fatty acids and biosynthesis of other metabolites. In addition to their central role in biochemical pathways, the mitochondria are important regulators of cell death. Pro-apoptotic proteins permeabilize the mitochondrial outer membrane, releasing cytochrome c (cyt c) to the cytosol. Cyt c initiates a series of proteolytic events carried out by caspases (4).

In *Drosophila dDP* mutants, cells fail to execute apoptosis following DNA damaging radiation. This defect was attributed to dysfunctional mitochondrial activity (3). It was shown that the genes required for mitochondrial biogenesis and activity are under the control of the dDP/dE2f1 complex. However, when endogenous *e2f1* gene is acutely removed in post-mitotic cells, they are sensitive to cell death induced by ionizing irradiation (3). This sensitivity to cell

death was permitted by functional mitochondria, suggesting that an acute inactivation of the dDP/dE2f1 complex is not sufficient to compromise mitochondrial activity.

In mammalian systems, phosphorylation of pRb by CDK4 and CDK6 is essential to release the inhibitory effect of pRb from E2Fs to activate the E2F-dependent transcriptional program. Inhibition of CDK4/6 leads to accumulation of active pRb, which acutely inactivates E2F and prevents induction of E2F-dependent transcription. PD0332991 is a small molecule drug that specifically inhibits the kinase activity of CDK4/6 and subsequently, robustly arrests cells in G1 phase (5). Paradoxically, pre-treatment with PD0332991 protected breast cancer cells from cell death induced by cytotoxic agents (6).

We hypothesized that acute inactivation of E2F by PD0332991 treatment results in changes in mitochondrial activity. We propose that modulation of mitochondrial activity by accumulation of active pRb plays an important role in sensitivity to cell death.

4.3. Results

A. PD0332991 potently arrests Rb-proficient cells in G1.

In order to address the effect of PD0332991 on mitochondria, we first confirmed that the treatment would result in a robust G1 arrest of Rb-proficient cells. We treated the normal breast tissue cells MCF10A, and two breast cancer cell lines, MCF7 and MDA-MB-231, with 500nM PD0332991 for 24 hours. The cell cycle profile assayed by DNA content clearly exhibited the disappearance of cells in S-phase and accumulation of cells in G1 (Fig. 15A-C). Consistent with the mechanism of action for PD0332991, the Rb-deficient MDA-MB-468 cells failed to arrest in G1 following PD0332991 treatment (Fig. 15D).

The combinatorial effect of PD0332991 and cytotoxic agents has been studied extensively in the Rb-proficient breast cancer cell line MDA-MB-231. The Knudsen group showed that the breast cancer cells pre-treated with PD0332991 were insensitive to either doxorubicin- or paclitaxel- induced apoptosis (6). Consistent with their observations, we also saw that PD0332991 pre-treatment blocked doxorubicin-induced arrest in S-phase (Fig. 15E). Additionally, the pretreatment blocked the accumulation of the apoptotic marker, cleaved PARP, in MDA-MB-231 cancer cell line (Fig. 15F).

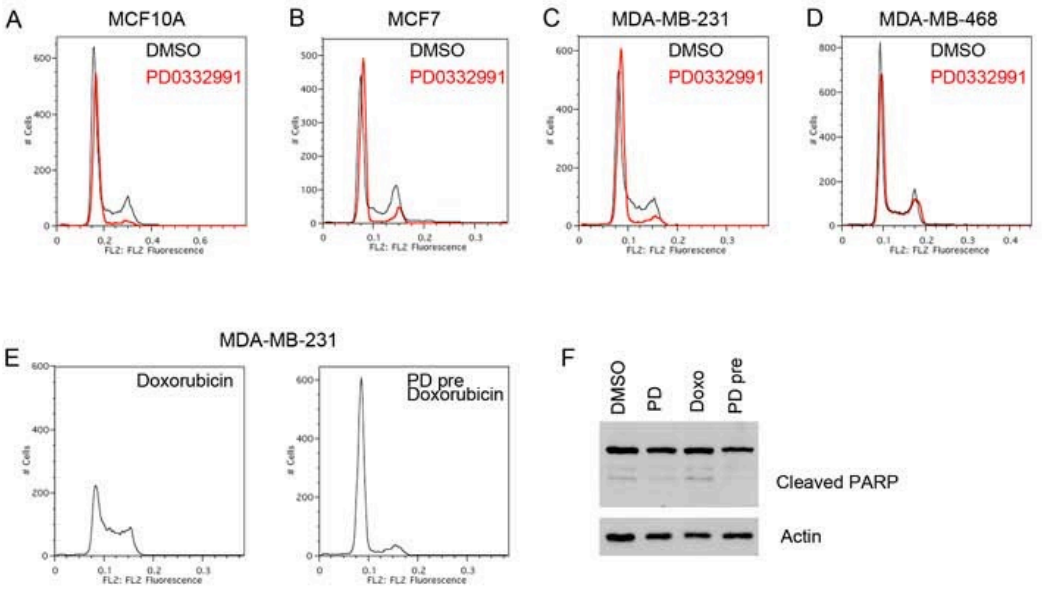

Figure 15. PD0332991 treatment arrests cells in G1.

(A-D) Cell cycle profile of breast tissue cells treated with 500nM PD0332991 (red trace) and control DMSO (black trace).
(E) MDA-MB-231 breast cancer cells treated with 1μM Doxorubicin alone for 24hr (left) and pre-treated with PD0332991 for 24hr and then subjected to doxorubicin treatment (right). Cell cycle profiles are visualized with Propidium Iodide staining.
(F) Western blot analysis of MDA-MB-231 cells assayed for apoptosis with the appearance of a band for cleaved PARP. Actin used as a loading control.

B. PD0332991 treatment increases mitochondrial activity of normal breast tissue MCF10A cells

We decided to first delineate the effect of PD0332991 treatment on the normal breast tissue cell line MCF10A. As shown previously, a 24hr treatment with PD0332991 arrests these cells in G1 (Fig. 16A). We reasoned that accumulation of active pRb would block E2f1 activity and subsequently, the expression of its target genes. We first measured the expression levels of previously defined mitochondria-associated genes, which are direct targets of the E2f1 transcription factor (3). We observed that the expression of these genes was either unchanged or increased (Fig. 16A). Because these cells are arrested in G1 and the classical E2f targets are required for G1 to S phase transition, we checked whether *PCNA* expression was affected. *PCNA* expression was downregulated consistent with the arrest in G1 (Fig. 16A). Therefore, the Rb-mediated increase in the mitochondria-associated gene expression may be conducted through an E2f-independent mechanism.

Next we asked whether this increase in the level of mitochondria-associated genes would result in an increase in oxidative phosphorylation. We measured oxygen consumption using the Seahorse Bioscience extracellular flux analyzer. Mitochonodrial activity is stressed with addition of a series of drugs. Oligomycin is injected which blocks ATP production, thus oxygen consumption. FCCP is an uncoupler of the membrane potential and therefore, allows for maximal production of ATP. Antimycin A and Rotenone are inhibitors of complex I and III, respectively, and block all mitochondrial respiration. This stress test gives an oxygen consumption profile, which can be compared between different treatments. A 24-hour treatment with PD0332991 boosted the basal oxygen consumption rate, consistent with the elevated

mitochondrial gene expression levels. Furthermore, these cells exhibited a much higher maximal respiration rate, which means that they have a larger reserve capacity should they need it.

C. Increased mitochondrial activity sensitized MCF10A cells to doxorubicin-induced apoptosis

Mitochondria play a central role in the execution of the apoptotic response (7). The release of cyt *c* from the inner membrane of the mitochondria triggers a cascade of signaling which results in programmed cell death. We asked whether increased mitochondrial activity in MCF10A cells following PD0332991 treatment was responsible for modulating apoptotic response. We employed Annexin V staining to measure apoptosis in cells treated with combinations of pharmaceutical drugs commonly used in the clinic. Annexin V is an antibody that selectively binds to phosphotidyl serines. During apoptosis, membrane phospholipid phosphotidyl serine is translocated from the inner layer of the plasma membrane to the outer leaflet, thereby exposing it to the extracellular space. Annexin V does not permeate intact cellular membrane; therefore will only bind to the exposed phosphotidyl serines and this serves as an early marker for apoptosis. Annexin V conjugated to FITC is measured by flow cytometry and the results are presented as histograms. The number of Annexin V-positive cells is quantified and presented as bar graphs.

Doxorubicin is a DNA-damaging agent that effectively induces apoptosis in cycling cells (8,9). We first measured the level of apoptosis following a 24hr treatment with 1μM doxorubicin in MCF10A cells. 27.9% of the total cells assayed were positive for Annexin V, compared to 14% basal level of cell death in the untreated culture (Fig. 16C, D). Pre-treatment with PD0332991 further sensitized the MCF10A cells to doxorubicin-induced apoptosis by dramatically increasing the Annexin V- positive cell percentage to 76.5% (Fig. 16C, D). If this

increase in sensitivity to apoptosis indeed is mediated through elevated mitochondrial activity and oxidative phosphorylation, then we should be able to recapitulate this effect by boosting oxidative phosphorylation by means other than PD0332991 treatment.

Bezafibrate is a pharmaceutical drug used for treatment of hyperlipidemia. It helps lower cholesterol and triglyceride levels in the blood (10). Bezafibrate is a pan-PPAR agonist that stimulates the expression of the genes required for beta-oxidation, products of which are fed into the TCA cycle and consequently, this boosts oxidative phosphorylation (11,12). Pre-treatment with 500 μM bezafibrate for 48 hours greatly sensitized the MCF10A cells to doxorubicin-induced apoptosis and resulted in a 71.9% Annexin V-positive cells. This result strongly supports that PD0332991-mediated increase in mitochondrial activity and oxidative phosphorylation is responsible for increased sensitivity to apoptosis. Pre-treating cells with both PD0332991 and bezafibrate even further increased the percentage of apoptotic cells to 82.9% (Fig. 16C).

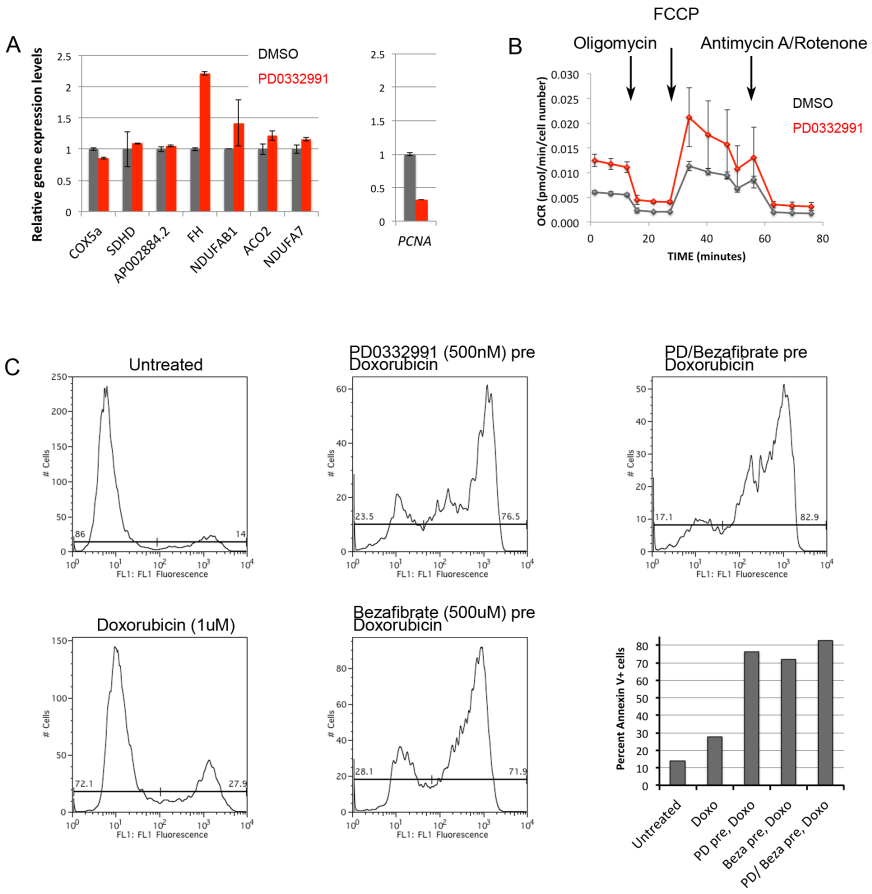

Figure 16. PD0332991 treatment of MCF10A cells enhances mitochondrial activity and sensitizes them to apoptosis.

(A) Relative gene expression levels measured by qRT-PCR. Mitochondria-associated genes on the left panel are increased or unaffected in PD0332991-treated cells (red bars) compared to DMSO control (gray bars). On the right, a decrease in PCNA gene expression in PD0332991-treated cells. Error bars indicate stdev of technical replicates. The data is representative of three independent experiments. The data is normalized to the reference gene *β2M* and presented relative to DMSO control.
(B) Oxygen consumption rate measured by the XF^{e}96 extracellular flux analyzer. The cells treated with 500nM PD0332991 for 24hr is presented in red, DMSO control in black. Data was normalized to cell number. Error bars indicate standard deviation of technical replicates. The data is representative of two independent experiments.
(C) Apoptosis measured by Annexin V-FITC staining in cells of indicated treatment. The left peak indicates the percentage of cells negative for Annexin V-FITC and the right peak indicates the percentage of cells positive for Annexin V-FITC (apoptotic). The quantification of Annexin V-FITC positive cell percentages is presented as a bar chart. The data is representative of two independent experiments.

D. PD0332991 treatment increases mitochondrial activity in breast cancer cell lines, MCF7 and MDA-MB-231, but they exhibit varying sensitivity to apoptosis

Based on the results we saw in normal breast tissue MCF10A cells, we reasoned that this increased sensitivity to apoptosis could be exploited to treat cancer cells. We subjected MCF7 and MDA-MB-231 cancer cells to PD0332991 treatment for 24 hours. As expected, both of these cell lines displayed elevated levels of E2f1 target mitochondria-associated genes and increased mitochondrial activity measured by the Seahorse Bioscience extracellular flux analysis (Fig. 17A-D). In MDA-MB-231 cells, the increase is particularly pronounced.

Similar to the MCF10A cells, we measured the sensitivity to doxorubicin-induced apoptosis in cancer cells. The histogram overlays for doxorubicin alone (gray shaded) and PD0332991 pre-treatment followed by doxorubicin (red) or with bezafibrate pre-treatment followed by doxorubicin (blue) are shown for each cell line. To our surprise, in MCF7 cells, pre-treatment with PD0332991 alone or bezafibrate alone showed no appreciable difference in doxorubicin-induced apoptosis (Fig. 17C). However, when MCF7 cancer cells were pre-treated with both PD0332991 and bezafibrate (green) simultaneously, the number of apoptotic cells increased by approximately two-fold. This result suggests that the higher resistance to cell death in MCF7 cancer cells, compared to normal MCF10A cells, had to be overcome with a combination of mechanisms that elevate mitochondrial activity. In the more aggressive breast cancer MDA-MB-231 cells, even the combination pre-treatment was not sufficient to further sensitize them to doxorubicin-induced apoptosis (Fig. 17G-H). These data taken together underline the inherent variability between cell lines and the level of resistance to cell death.

To confirm that the PD0332991-mediated effects are Rb-dependent, we performed the same experiments on Rb-null breast cancer MDA-MB-468 cell line. As expected, the expression

levels for mitochondria-associated genes were unaffected (Fig. 18A). Consequently, there was no significant change in oxidative phosphorylation and no effect on the level of doxorubicin-induced apoptosis (Fig. 18B-D).

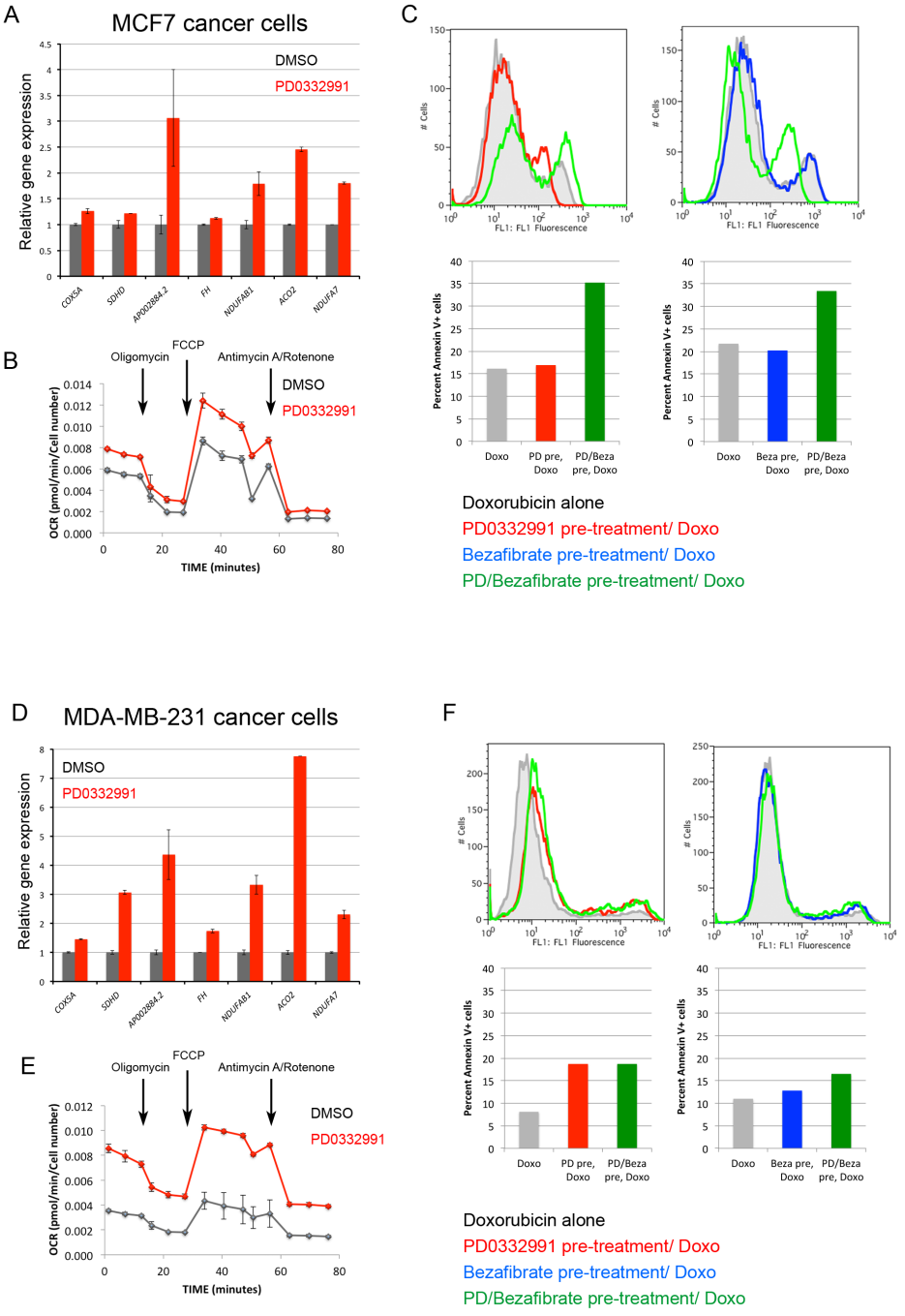

Figure 17. Breast cancer cell lines treated with PD0332991 exhibit enhanced mitochondrial activity, but differential sensitivity to apoptosis.

(A, D) Relative gene expression levels measured by qRT-PCR. Mitochondria-associated genes on the left panel are increased or unaffected in PD0332991-treated cells (red bars) compared to

DMSO control (gray bars). The data is normalized to the reference gene *β2M* and presented relative to DMSO control.
(B, E) Oxygen consumption rate measured by the XF^{e}96 extracellular flux analyzer. The cells treated with 500nM PD0332991 for 24hr is presented in red, DMSO control in black. Data was normalized to cell number. Error bars indicate standard deviation of technical replicates. The data is representative of two independent experiments.
(C, F) Apoptosis measured by Annexin V-FITC staining in cells of indicated treatment. The gray shaded peaks correspond to 1μM doxorubicin treatment alone, red trace to PD0332991 treatment, blue trace to 500 μM bezafibrate treatment and the green trace to the concurrent treatment of both PD0332991 and bezafibrate. The quantification of Annexin V-FITC positive cell percentages is presented as a bar chart. The data is representative of two independent experiments.

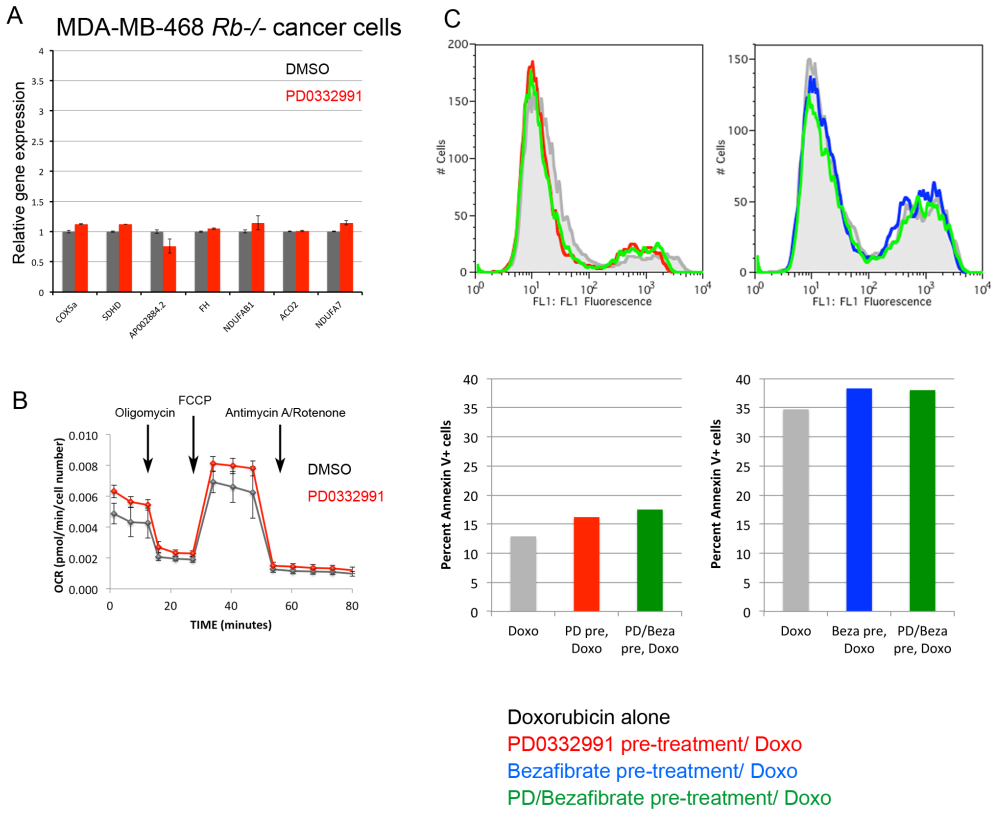

Figure 18. *Rb-null* MDA-MB-468 cells are insensitive to PD0332991 treatment.

(A, D) Relative gene expression levels measured by qRT-PCR. Mitochondria-associated genes on the left panel are increased or unaffected in PD0332991-treated cells (red bars) compared to DMSO control (gray bars). The data is normalized to the reference gene *β2M* and presented relative to DMSO control.
(B, E) Oxygen consumption rate measured by the XF^{e}96 extracellular flux analyzer. The cells treated with 500nM PD0332991 for 24hr is presented in red, DMSO control in black. Data was normalized to cell number. Error bars indicate standard deviation of technical replicates. The data is representative of two independent experiments.
(C, F) Apoptosis measured by Annexin V-FITC staining in cells of indicated treatment. The gray shaded peaks correspond to 1μM doxorubicin treatment alone, red trace to PD0332991 treatment, blue trace to 500 μM bezafibrate treatment and the green trace to the concurrent treatment of both PD0332991 and bezafibrate. The quantification of Annexin V-FITC positive cell percentages is presented as a bar chart. The data is representative of two independent experiments.

4.4. Discussion

In the clinic, the prevailing question is why some cancer patients respond well to a treatment, while others don't. Simply put, why do some treatments kill cancer cells and others don't. This differential response depends on many factors with all upstream signaling converging on the apoptotic pathway, which is mediated through mitochondria.

In our studies here, we describe the effect of the CDK4 inhibitor, PD0332991, on mitochondrial activity in breast cancer cell lines. In addition to potently arresting cells in G1 in an Rb-dependent fashion, PD0332991 treatment also elevated mitochondria-associated gene expression levels as well as oxidative phosphorylation. The increase in gene expression was counterintuitive given the inhibitory effect of pRb on E2f1 transcription factor. However, the classical target *PCNA* gene expression was reduced consisted with the cell cycle arrest (Fig. 16A). This result suggests that pRb is functioning as an activator or as a de-repressor of mitochondria-associated gene expression in an E2f-independent fashion. The latter possibility is likely according to a recent study demonstrating that pRb antagonizes histone demethylase Kdm5 during myogenic differentiation (13). The study demonstrated that mitochondrial activity is necessary and sufficient for differentiation of mouse embryonic fibroblasts (MEF) into myotubes. In MEFs, mitochondria-associated genes are bound and silenced by Kdm5. Kdm5 on these genes is replaced by pRb as MEFs differentiate into myotubes, strongly suggesting that pRb binding relieves the inhibition imposed by Kdm5.

We argue that an increase in mitochondrial activity and oxygen consumption induced by PD0332991 sensitizes cells to apoptosis. However, this sensitivity varies from one cell type to another. In normal MCF10A cells, pre-treatment with PD0332991 results in a very high sensitivity to doxorubicin-induced apoptosis. MCF7 cancer cells required the combined effect of

PD0332991 and bezafibrate to achieve a high level of doxorubicin- induced apoptosis. MDA-MB-231 cells derived from an aggressive basal subtype of breast cancer were even more insensitive to pro-apoptotic stimuli. All three cell lines exhibited different thresholds for cell death despite increased levels of mitochondria-associated gene levels and mitochondrial activity in all of them.

Interestingly, in several types of cancers, such as multiple myeloma, acute lymphocytic leukemia, ovarian cancer and acute myeloid leukemia, it has been shown that the differential response to treatment was dependent on mitochondrial priming (14). Mitochondrial priming is defined as "*the magnitude of response of mitochondria to pro-apoptotic peptides derived from the BH3 domains of the pro-apoptotic BH3-only proteins"* (as quoted from (14)). It is measured by the amount of cyt *c* released or the loss of mitochondrial membrane potential following a treatment with BH3 peptides. The greater the loss of mitochondrial membrane potential in response to the pro-apoptotic peptide treatment, the higher the number of cells primed for cell death. Furthermore, in AML, mitochondrial priming determined not only initial response to cytotoxic chemotherapy, but also the risk of relapse (15). This kind of analysis has been done in leukemia and lymphoma only, but in principle, this idea of mitochondrial priming could expand to a wider array of cancer types (16). Low mitochondrial priming in breast cancer cells compared to the normal MCF10A line could be responsible for their increased resistance to cell death.

Our results describe the role of the pRb in response to cytotoxic drug treatments of breast cancer cells. We showed that pRb-induced enhanced mitochondrial activity is sufficient to sensitize the normal MCF10A cells and, in conjunction with bezafibrate, MCF7 cancer cells to apoptosis. We show that the aggressive MDA-MB-231 breast cancer cells are inherently more resistant to apoptosis. With the assays and methods established in the lab, it is imperative to

extend this analysis to the Hippo pathway and ask whether it cooperates with Rb in regulation of the mitochondrial activity and subsequently, the apoptotic response.

4.5. Materials and Methods

A. Cell culture

MCF7, MDA-MB-231 and MDA-MB-468 cells were maintained in DMEM supplemented with 10% fetal bovine serum. MCF10A cells were grown in DMEM/F-12 medium supplemented with 5% horse serum, 0.02 μg/ml EGF, 0.5 μg/ml hydrocortizone, 0.01 mg/ml, 10μg/ml cholera toxin, 100 units/ml penicillin/streptomycin. All cultures were maintained at 37^{o}C and 5% CO_2.

B. Drug treatments

The cells were plated at 2x10^5 cells/well density in 6-well plates and allowed to adhere overnight. The drugs were added at the following concentrations: [PD0332991]= 500nM, [Doxorubicin]= 1μM, [Bezafibrate]= 500μM in 2ml volume. 0.1% DMSO treatment was used as a control.

C. Gene expression qRT-PCR

Cells of designated drug treatments were lysed in 1ml TRIzol (ThermoFisher) per one well of a 6-well plate. The RNA was re-suspended in 50 μl of molecular grade water. 500ng of total RNA was used for the Reverse Transcriptase PCR reactions (SensiFAST cDNA synthesis kit, Bioline). 1:20 dilution and SensiFAST Real-Time PCR kits were used for Quantitative Real-Time PCR reaction on Roche LightCycler 480 using primers previously published in Ambrus A *et al* (2014).

D. Flow Cytometry

For Propidium Iodide (PI) cell cycle profile assays, the cells of designated treatments were harvested and fixed in 95% EtOH overnight at 4°C. The fixed cells were stained with 50 μg/ml Propidium Iodide (Sigma P4170-10MG). Annexin V staining was performed using FITC-conjugated Annexin V antibody (BD Pharmingen 556547) according to the manufacturer's instructions. All flow cytometry data were analyzed using FlowJo 9.3.2 software (Ashland, OR).

E. Mito Stress Test Assay

The cells treated with PD0332991 were counted and plated to Seahorse Biosciences assay plate at $2x10^4$ cells per well. After 24hr, the Mito Stress Assay was run according to the manufacturer's recommended protocol. The results were normalized to number of cells per well. Drug injections were set at the following final concentrations: [FCCP]= 0.5μM, [Oligomycin]= 2μM, [Rotenone/Antimycin A]= 0.5μM.

F. Western Blot

Cells of indicated treatments were lysed in RIPA buffer. 30μg of total protein was loaded per well for SDS-PAGE. Rabbit anti- cleaved PARP antibody (Cell Signaling, Cat No 9541) was used at 1:3000 concentration in 5% BSA, incubated for 2 hours at RT. Mouse anti- actin antibody was used for loading control, incubated for 2 hours at RT.

4.6. Literature cited

1. Nagaraj R, Gururaja-Rao S, Jones KT, Slattery M, Negre N, Braas D, et al. Control of mitochondrial structure and function by the Yorkie/YAP oncogenic pathway. Genes Dev. 2012 Sep 17;26(18):2027–37.

2. Benevolenskaya EV, Frolov MV. Emerging Links between E2F Control and Mitochondrial Function. Cancer Research. American Association for Cancer Research; 2015 Jan 29.

3. Ambrus AM, Islam ABMMK, Holmes KB, Moon NS, Lopez-Bigas N, Benevolenskaya EV, et al. Loss of dE2F Compromises Mitochondrial Function. Developmental Cell. Elsevier Inc; 2013 Nov 25;27(4):438–51.

4. Westermann B. Mitochondrial fusion and fission in cell life and death. Nature Publishing Group. Nature Publishing Group; 2010 Dec 1;11(12):872–84.

5. Toogood PL, Harvey PJ, Repine JT, Sheehan DJ, VanderWel SN, Zhou H, et al. Discovery of a potent and selective inhibitor of cyclin-dependent kinase 4/6. J Med Chem. 2005 Apr 7;48(7):2388–406.

6. Dean JL, McClendon AK, Knudsen ES. Modification of the DNA Damage Response by Therapeutic CDK4/6 Inhibition. Journal of Biological Chemistry. 2012 Aug 17;287(34):29075–87.

7. Detmer SA, Chan DC. Functions and dysfunctions of mitochondrial dynamics. Nat Rev Mol Cell Biol. 2007 Nov;8(11):870–9.

8. Kurz EU, Douglas P, Lees-Miller SP. Doxorubicin activates ATM-dependent phosphorylation of multiple downstream targets in part through the generation of reactive oxygen species. Journal of Biological Chemistry. American Society for Biochemistry and Molecular Biology; 2004 Dec 17;279(51):53272–81.

9. MD AM-A, MD EAP. Anthracycline- and/or taxane-resistant breast cancer: Results of a literature review to determine the clinical challenges and current treatment trends. Clinical Therapeutics. Excerpta Medica Inc; 2009 Aug 1;31(8):1619–40.

10. Goldenberg I, Benderly M, Goldbourt U. Update on the use of fibrates: focus on bezafibrate. Vasc Health Risk Manag. 2008;4(1):131–41.

11. Bastin J, Aubey F, Rötig A, Munnich A, Djouadi F. Activation of Peroxisome Proliferator-Activated Receptor Pathway Stimulates the Mitochondrial Respiratory Chain and Can Correct Deficiencies in Patients' Cells Lacking Its Components. The Journal of Clinical Endocrinology & Metabolism. 2008 Apr;93(4):1433–41.

12. Noe N, Dillon L, Lellek V, Diaz F, Hida A, Moraes CT, et al. Bezafibrate improves mitochondrial function in the CNS of a mouse model of mitochondrial encephalopathy. Mitochondrion. 2013 Sep;13(5):417–26.

13. Váraljai R, Islam ABMMK, Beshiri ML, Rehman J, Lopez-Bigas N, Benevolenskaya EV. Increased mitochondrial function downstream from KDM5A histone demethylase rescues differentiation in pRB-deficient cells. Genes Dev. 2015 Sep 4;29(17):1817–34.

14. Ni Chonghaile T, Sarosiek KA, Vo T-T, Ryan JA, Tammareddi A, Moore VDG, et al. Pretreatment mitochondrial priming correlates with clinical response to cytotoxic chemotherapy. Science. 2011 Nov 25;334(6059):1129–33.

15. Vo T-T, Ryan J, Carrasco R, Neuberg D, Rossi DJ, Stone RM, et al. Relative Mitochondrial Priming of Myeloblasts and Normal HSCs Determines Chemotherapeutic Success in AML. Cell. Elsevier; 2012 Oct 12;151(2):344–55.

16. Ryan JA, Brunelle JK, Letai A. Heightened mitochondrial priming is the basis for apoptotic hypersensitivity of CD4+ CD8+ thymocytes. Proc Natl Acad Sci USA. National Acad Sciences; 2010 Jul 20;107(29):12895–900.

5. Concluding remarks

5.1. The Hippo pathway transcriptional mechanism

The Hippo signaling pathway regulates organ size by controlling the activity of the transcriptional co-activator Yki. Despite a tremendous leap in our understanding of the Hippo pathway, we still do not fully comprehend the transcriptional mechanisms of Yki. In *Drosophila,* Yki is recruited to its target genes by DNA-binding proteins, such as TEAD/TEF family protein Scalloped (Sd), the homeodomain protein Homothorax (Hth) and the zinc-finger transcription factor Teashirt (Tsh) (1-3). The interaction with the Dpp pathway is also mediated through Yki. In this particular case, downstream effectors of both pathways, Yki and Mad, physically associate and bind to their target miRNA *bantam* to synergistically promote growth (4).

We uncovered a novel mode of interaction between the Hippo and Rb pathways. The downstream transcription factor complexes, dE2f1/dDP and Yki/Sd, activate the expression of their common target genes. In *Nicolay BN, Bayarmagnai B et al (2011),* I demonstrated that these complexes directly bind to the promoters of cell cycle targets, such as *DNA pol ε, dDp and Mcm10* (5). Our further analysis in *Bayarmagnai B et al (2012)* identified chromatin-binding protein GAGA Factor (GAF), which is encoded by the *Trithorax-like (Trl)* gene, as a novel and critical partner in transcriptional regulation by Yki/Sd and dE2f1 (6). I showed that functional GAF and its binding to the promoters of target genes common to dE2f1-Yki/Sd was required for both normal developmental and ectopic cell proliferation. Mechanistically, GAF forms a multi-protein complex with RBF and E2f1. The Irvine group demonstrated that GAF also forms a complex with Yki/Sd (7). Preliminary results of the fast protein liquid chromatography (FPLC) experiments indicate that RBF, E2f1 and GAF are eluted in the same fraction further supporting the existence of a native multi-protein complex. We propose that GAF is the bridging molecule

that facilitates the interaction between dE2f1/dDP and Yki/Sd complexes and relieves the repression imposed by RBF. Furthermore, GAF has been shown to promote nucleosome-free regions, facilitate DNA looping and recruit RNA Pol II (8,9). This interaction provides an elegant mechanism for the Rb and Hippo pathways to cooperatively regulate transcription.

Such regulation of transcription by the Rb and Hippo pathways is conserved in mammalian systems, including humans. It adds to the overwhelming amount of evidence of their implication in human developmental processes and pathologies. In cancers, both genetically and functionally, the Rb pathway is most targeted. Evidence for the amplification of YAP and silencing of the tumor suppressor kinases in human cancers are emerging with alarming speed (10,11). The requirement for the cooperation of the Rb and Hippo pathways has been demonstrated in pancreatic ductal adenocarcinoma. Oncogenic *Kras* drove the formation of the initial tumor, however the tumor relapsed even after *Kras* expression was extinguished. The surviving cancer cells re-emerged by exploiting a different mechanism of upregulating cell cycle genes by YAP and E2f (12).

These data collectively underscore the importance of halting the Hippo pathway transcriptional output in human pathologies and the study presented in this thesis provides more insight into the mechanism and identification of novel targets.

5.2. Rb and Hippo pathways as guardians of terminal differentiation

It has been well established that a terminally differentiated cell is much more plastic than previously thought (13). On one hand, for tissue homeostasis and maintenance of functionality, cells need to undergo proliferation or dedifferentiation to make up for the lost cells, especially following a mechanical damage or injury (14). This ability, on the other hand, can be a curse. If

cell proliferation is uncontrolled, it can lead to benign or malignant tumors. An intricate balance must be maintained and we still don't have a full understanding of the mechanisms involved.

The work presented here describes a novel setting of a defect in maintaining differentiation. With the powerful genetic model of *Drosophila* eye imaginal disc and the marker analysis, we demonstrated that concurrent inactivation of the Hippo and Rb pathways result in loss of differentiation markers (5). Importantly, we revealed that this defect is independent of their role in proliferation. Additionally, this crosstalk occurs at the level of tumor suppressors RBF and Wts or Hpo, as I showed that over-expression of *yki* in the progenitor eye cells in the *rbf* mutant background is not sufficient to trigger differentiation defects (Fig. 12).

Addressing such complex phenotypes requires high precision and resolution methods. Analyzing bulk samples and whole tissues are no longer feasible when the cells of interest can be easily obscured in a heterogeneous population. Therefore, I created the genetic lineage-tracing tool and optimized the conditions for single cell analysis to determine the mechanism by which Rb and Hippo pathways cooperatively guard the state of terminal differentiation.

The eye tissue containing clones of *rbf wts* cells were dissociated into single cells and captured in individual wells. Initial analysis confirmed the success of our approach and identified differentiated cells marked by the expression of the reporter gene *lacZ* (Fig. 14). Furthermore, the current experiments of single cell RNA sequencing will give insight into the precise transcriptional signature of the *rbf wts* double mutant cells. This work is at an exciting stage where all groundwork for precise analysis has been completed. We are finally able to specifically identify and characterize the cells that fail to maintain the expression of their differentiated identity.

Although the role of the Hippo pathway is well established in cell proliferation and organ growth, a new previously uncharacterized role in cell fate maintenance is emerging from the works of our lab and others. Most notably, the Hippo has been shown to be critical for hepatocyte fate maintenance in cooperation with the Notch pathway (15). These studies also highlight the significance of studying the cooperation among pathways, as no pathway functions in isolation. By focusing on one pathway at a time, we are bound to miss their roles critical for normal physiology and human pathologies.

5.3. Literature cited

1. Goulev Y, Fauny JD, Gonzalez-Marti B, Flagiello D, Silber J, Zider A. SCALLOPED Interacts with YORKIE, the Nuclear Effector of the Hippo Tumor-Suppressor Pathway in Drosophila. Current Biology. 2008 Mar;18(6):435–41.

2. Zhang T, Zhou Q, Pignoni F. Yki/YAP, Sd/TEAD and Hth/MEIS Control Tissue Specification in the Drosophila Eye Disc Epithelium. Bergmann A, editor. PLoS ONE. 2011 Jul 19;6(7):e22278.

3. Peng HW, Slattery M, Mann RS. Transcription factor choice in the Hippo signaling pathway: homothorax and yorkie regulation of the microRNA bantam in the progenitor domain of the Drosophila eye imaginal disc. Genes Dev. 2009 Oct 1;23(19):2307–19.

4. Oh H, Irvine KD. Cooperative Regulation of Growth by Yorkie and Mad through bantam. Developmental Cell. Elsevier; 2011 Jan 18;20(1):109–22.

5. Nicolay BN, Bayarmagnai B, Moon NS, Benevolenskaya EV, Frolov MV. Combined inactivation of pRB and hippo pathways induces dedifferentiation in the Drosophila retina. PLoS Genet. 2010 Apr;6(4):e1000918.

6. Bayarmagnai B, Nicolay BN, Islam ABMMK, Lopez-Bigas N, Frolov MV. Drosophila GAGA factor is required for full activation of the dE2f1-Yki/Sd transcriptional program. cc. 2012 Nov 15;11(22):4191–202.

7. Oh H, Slattery M, Ma L, Crofts A, White KP, Mann R, et al. Genome-wide Association of Yorkie with Chromatin and Chromatin-Remodeling Complexes. CellReports. The Authors; 2013 Feb 6;:1–10.

8. Mahmoudi T, Katsani KR, Verrijzer CP. GAGA can mediate enhancer function in trans by linking two separate DNA molecules. The EMBO Journal. 2002 Apr 2;21(7):1775–81.

9. Fuda NJ, Guertin MJ, Sharma S, Danko CG, Martins AL, Siepel A, et al. GAGA Factor Maintains Nucleosome-Free Regions and Has a Role in RNA Polymerase II Recruitment to Promoters. Lieb JD, editor. PLoS Genet. 2015 Mar 27;11(3):e1005108–22.

10. Pan D. The Hippo Signaling Pathway in Development and Cancer. Developmental Cell. Elsevier Inc; 2010 Oct 19;19(4):491–505.

11. Harvey KF, Zhang X, Thomas DM. The Hippo pathway and human cancer. Nature Publishing Group; 2013 Mar 7;:1–12.

12. Oncogene ablation-resistant pancreatic cancer cells depend on mitochondrial function. Nature Publishing Group; 2015 Apr 9;514(7524):628–32.

13. Takahashi K, Yamanaka S. Induction of Pluripotent Stem Cells from Mouse Embryonic and Adult Fibroblast Cultures by Defined Factors. Cell. 2006 Aug;126(4):663–76.

14. Jessen KR, Mirsky R, Arthur-Farraj P. The Role of Cell Plasticity in Tissue Repair: Adaptive Cellular Reprogramming. Developmental Cell. Elsevier Inc; 2015 Sep 28;34(6):613–20.

15. Yimlamai D, Christodoulou C, Galli GG, Yanger K, Pepe-Mooney B, Gurung B, et al. Hippo Pathway Activity Influences Liver Cell Fate. Cell. Elsevier Inc; 2014 Jun 5;157(6):1324–38.

Battuya Bayarmagnai

Department of Biochemistry and Molecular Genetics
University of Illinois at Chicago
900 S. Ashland Avenue, Room 2360
Chicago, IL 60607

Phone: 307-220-3911
Email: bbayar2@uic.edu

Education

2008-Present — **University of Illinois at Chicago**, Chicago, IL
Candidate for PhD in Biochemistry & Molecular Genetics

2004-2008 — **University of Wyoming**, Laramie, WY
Bachelor of Science, Molecular Biology

Peer-Reviewed Publications

1. **Bayarmagnai B**, Nicolay BN, Islam ABMMK, Lopez-Bigas N, Frolov MV. *Drosophila GAGA Factor is required for the full activation of dE2f1-Yki/Sd transcriptional program.* Cell Cycle. 2012 vol. 11 (22) pp. 4191 – 4202.

   Image from the manuscript was featured on the cover of vol.11 (22) issue of Cell Cycle.

2. Nicolay BN, **Bayarmagnai B**, Islam ABMMK, Lopez-Bigas N, Frolov MV. *Cooperation between dE2f1 and Yki/Sd defines a distinct transcriptional program necessary to bypass cell cycle exit*. Genes & Development. 2011 vol. 25 (4) pp. 323-335.

3. Nicolay BN, **Bayarmagnai B**, Moon N.-S., Benevolenskaya EV, Frolov MV. *Combined inactivation of pRb and Hippo pathways induces dedifferentiation in the Drosophila retina*. PLoS Genetics. 2010 vol. 6 (4) e1000918.

4. Choresh O, **Bayarmagnai B**, Lewis RV. *Spider web glue: two proteins expressed from the opposite strands of the same DNA sequence*. Biomacromolecules. 2009 vol. 10 (10) pp. 2852-2856.

Research Experience

PhD Thesis Research — **University of Illinois at Chicago**
(5/2009- Present)
Advisor: Maxim V. Frolov

Project 1: Understanding the interaction between the RB and Hippo tumor suppressor pathways in *Drosophila*.

1. Demonstrated that the downstream effectors of the RB and Hippo pathways, dE2f1 and Yki, interact with a DNA-binding protein, GAGA Factor, to fully activate their target genes required for cell proliferation. (Published in *Cell Cycle*).

2. Examining the mechanism by which the RB and Hippo pathways maintain the differentiated state of cells during development in *Drosophila*. Cloned and generated a novel cell labeling system to trace the dedifferentiated cells *in vivo*.

Project 2: Studying the effect of the CycD/CDK4 inhibitor PD0332991 on cellular metabolism in breast cancer cells.

Undergraduate Research **University of Wyoming**
(8/2006- 5/2008)
Advisors: Omer Choresh/Randolph Lewis

1. Cloned a novel gene encoding biological glue in orb-weaving spider, *Arrenius gemmoides*.

2. Demonstrated that the gene contains highly repetitive sequences that are 95% identical to the homologous gene from another orb-weaving spider species, *Nephila clavipes*. (Published in *Biomacromolecules*)

Awards/Fellowships

Western Heritage Scholarship	2004-08
NSF Wyoming EPSCoR Undergraduate Research Fellowship	2007
International Student Scholarship	2006
NSF Wyoming EPSCoR Undergraduate Summer Research Fellowship	2006
NSF Wyoming EPSCoR Undergraduate Freshman Research Fellowship	2005
University of Wyoming Dean's and President's Honor Roll	2004-05

Poster and Oral Presentations

"Following dedifferentiation in cells with inactivated Rb and Hippo pathways", *Chicago Symposium on Cell Signaling*, May 2015 (Poster)

"Following dedifferentiation in cells with inactivated Rb and Hippo pathways", Genetics Society of America *Drosophila Research Conference*, March 2015 (Poster)

"Rb and Hippo tumor suppressor pathways cooperate to regulate cell proliferation and differentiation", *Cancer Center Research Forum*, UIC, April 2013 (Poster)

"Rb and Hippo tumor suppressor pathways cooperate to regulate cell proliferation and differentiation", *College of Medicine Research Forum*, UIC, November 2013 (Poster)

"The role of the RBF and Hippo pathways in organ growth in *Drosophila*", *International Congress of Young Biologists- SymBioSE Russia*, Irkutsk, Russia, August 2013 (Oral)

"Drosophila GAGA Factor is required for full activation of target genes common to dE2f1 and Yki/Sd", Genetics Society of America *Drosophila Research Conference*, Chicago, March 2012 (Poster)

"The role of GAGA Factor in Yki-mediated cell proliferation", *Biochemistry and Molecular Genetics Departmental Retreat*, October 2011 (Poster)

"Screen to identify tumor suppressors that interact with RBF/dE2f1", *Biochemistry and Molecular Genetics Departmental Retreat*, October 2009 (Poster)

Teaching and Training Experience

1. Teaching assistant: Medical Biochemistry and Nutrition (BMS648)

2. Successfully completed course: Foundations of College Teaching (GC593)

3. Training of rotation students